



1 The Network for the Detection of Atmospheric Composition 2 Change at 35 Years: Achievements and Future Strategy.

3

4 Irina Petropavlovskikh^{1,2}, Martine De Mazière³, Anne M. Thompson^{4,5}, Jeannette D. Wild^{6,7}, James
5 W. Hannigan⁸, Henry B. Selkirk⁹, Reem A. Hannun¹⁰, Wolfgang Steinbrecht¹¹, Jean-Christopher
6 Lambert³, Roeland Van Malderen¹², Elizabeth Asher^{1,2}, Raul R. Cordero^{13,14}, Sophie Godin-
7 Beekmann¹⁵, Daan Hubert³, Sergey Khaykin¹⁵, Karin Kreher¹⁶, Thierry Leblanc¹⁷, Emmanuel
8 Mahieu¹⁸, Eliane Maillard Barras¹⁹, Glen McConville^{1,2}, Gerald Nedoluha²⁰, Ivan Ortega⁸, Alberto
9 Redondas Marrero²¹, Gunther Seckmeyer²², Ryan M. Stauffer⁴, Sarah A. Strode^{4,23}, Kim Strong²⁴,
10 Takafumi Sugita²⁵, Michel Van Roozendael³, Voltaire Velazco¹¹, Corinne Vigouroux³, Baerbel
11 Vogel²⁶

12

13 ¹CIRES, University of Colorado, Boulder, CO USA

14 ²NOAA, Global Monitoring Lab, Boulder, CO, USA

15 ³Royal Belgian Institute for Space Aeronomy (BIRA-IASB), Brussels, Belgium

16 ⁴Atmospheric Chemistry and Dynamics Laboratory, NASA Goddard Space Flight Center, Greenbelt, MD, USA

17 ⁵University of Maryland, Baltimore County, Baltimore, MD, USA

18 ⁶Earth System Science Interdisciplinary Center (ESSIC/CISESS), University of Maryland, College Park, MD, USA

19 ⁷NOAA/NESDIS/Center for Satellite Applications and Research (STAR), College Park, MD, USA

20 ⁸National Center for Atmospheric Research, Boulder, CO, USA

21 ⁹Agile Decision Support, NASA Headquarters, Washington, DC USA

22 ¹⁰Atmospheric Science Branch, NASA Ames Research Center, Moffett Field, CA USA

23 ¹¹Deutscher Wetterdienst - German Weather Service, Hohenpeissenberg, Germany

24 ¹²Royal Meteorological Institute of Belgium, Solar-Terrestrial Centre of Excellence, Uccle, Belgium

25 ¹³RUG, University of Groningen, Wirdumerdijk 34, 8911 CE Leeuwarden, The Netherlands

26 ¹⁴USACH, Universidad de Santiago de Chile. Av. Bernardo O'Higgins 3363, 9170022 Santiago, Chile.

27 ¹⁵LATMOS/IPSL, CNRS, Sorbonne Université, UVSQ, Paris, France

28 ¹⁶BK Scientific GmbH, Mainz, 55130, Germany

29 ¹⁷Jet Propulsion Laboratory, California Institute of Technology, Wrightwood, California, USA

30 ¹⁸Department of Astrophysics, Geophysics and Oceanography, UR SPHERES, University of Liège, Liège, Belgium

31 ¹⁹Federal Office of Meteorology and Climatology MeteoSwiss, Payerne, Switzerland

32 ¹⁰Remote Sensing Division, Naval Research Laboratory, Washington, DC, USA

33 ²¹Izaña Atmospheric Research Center, Agencia Estatal de Meteorología, 38001 Santa Cruz, Tenerife, Spain

34 ²²Leibniz University of Hannover/Institute of Meteorology, 30419 Hannover, Germany

35 ²³Morgan State University, GESTAR-II, Baltimore, MD, USA

36 ²⁴Department of Physics, University of Toronto, Toronto, ON, Canada

37 ²⁵National Institute for Environmental Studies (NIES), Tsukuba, Ibaraki, Japan

38 ²⁶Institute of Climate and Energy Systems (ICE-4), Forschungszentrum Jülich, Jülich, Germany

39

40 Correspondence to Irina Petropavlovskikh (irina.petropavlovskikh@colorado.edu), Anne Thompson
41 (amthomp1@umbc.edu), Martine DeMazier (martinedemazi@gmail.com)

42

43 **Abstract.** Since 1991, continuous, consistently calibrated and openly archived ground-based measurements from the
44 Network for the Detection of Atmospheric Composition Change (NDACC) have been collected to investigate processes
45 responsible for decadal-scale changes, anomalies in atmospheric composition, and to validate satellite observations and



46 model simulations. These measurements, from nearly 120 stations, support fundamental research in the area of
47 stratospheric and tropospheric processes impacting ozone chemistry, greenhouse gases, atmospheric radiative forcing,
48 air quality, and interactions with solar radiation and the entire Earth system. NDACC data are supplemented by
49 observations from 11 global Cooperating Networks. The operational principles of Cooperating Networks are well aligned
50 with NDACC objectives and protocols, focusing on data that (a) are high-quality, uniformly processed and traceable to
51 reference standards; and (b) capture short-term (daily to interannual) anomalies and long-term trends. This paper
52 summarizes the NDACC organizational structure. We review the major accomplishments of NDACC since De Mazière
53 et al. (2018), collaborative research with Cooperating Networks, and interactions with the satellite and modeling
54 communities. Ground-based atmospheric composition monitoring is at a crossroads. Challenges include sustainability of
55 human and financial resources required for complex and intensive data collection, technical issues including aging
56 instrumentation, requirements for FAIR (findable, accessible, interoperable, reusable) data, and lack of data over most
57 of Asia, Africa and South America. NDACC is well-positioned to adopt a three-pronged strategy going forward:
58 protecting and modernizing existing stations; promoting the growing use of NDACC data; expanding the number of
59 measured species and network coverage in under-sampled or under-reporting regions.

60

61 1 Introduction

62 As an integral part of the global observing system, the overriding goal of the Network for Detection of Atmospheric
63 Composition Change (NDACC) has been to collect and maintain high-quality ground-based data – both remote-sensing
64 and *in situ* – in order to detect changes and trends in atmospheric composition and to understand the impacts of these
65 changes on the mesosphere, stratosphere, and troposphere. NDACC first emerged as the Network for Detection of
66 Stratospheric Change (NDSC) in the late 1980s and became operational in 1991 (Kurylo et al, 2016). The network was
67 given its present title in 2006, reflecting research support beyond the stratosphere. The network extended selected
68 measurements into the mesosphere to understand its chemical and physical state as well as into the troposphere to study
69 processes impacting air quality and the climate.

70 As the network extended its vertical domain, the objectives expanded and are currently:

- 71 ▪ Establish long-term databases to detect changes and trends in atmospheric composition and to understand their
72 impacts on mesosphere, stratosphere and troposphere;
- 73 ▪ Establish scientific links and feedbacks among changes in atmospheric composition, climate, and air quality;
- 74 ▪ Validate and merge atmospheric measurements from other platforms (i.e., satellites, aircraft and ground-based
75 platforms);
- 76 ▪ Provide critical data sets to help fill gaps in satellite observations;
- 77 ▪ Provide collaborative support to scientific field campaigns and to other chemistry and climate-observing
78 networks;
- 79 ▪ Provide validation and development support for atmospheric models;
- 80 ▪ Contribute to assessments of the state of the atmosphere (WMO/UNEP, IGAC, IPCC, etc.).



81 The last objective was added in 2024, following the recognition of its importance as a fundamental contribution to the
82 NDACC since its establishment.
83 De Mazière et al. (2018) provided a brief history of the network, reviewed major accomplishments during its first 25
84 years of operation, and discussed recent developments and challenges. Their paper emphasized that NDACC must update
85 its capabilities as new data needs arise. They highlighted developments that could enable NDACC to meet its objectives
86 going forward. In the seven years since *De Mazière et al.* (2018) the need for the network enhancements has become
87 urgent. *Salawitch et al.* (2025) described a train of unexpected geophysical events, both natural and human-induced, that
88 have led to substantial anomalies in stratospheric composition. They point out that our understanding of the scale, extent,
89 and timing of these disturbances was made possible by robust, comprehensive global-scale observations by the
90 Microwave Limb Sounder (MLS) on the Aura satellite and the Atmospheric Chemistry Experiment-Fourier Transform
91 Spectrometer (ACE-FTS) on SCISAT since the early 2000s. However, our global scale capability to observe upper
92 atmospheric composition will be drastically reduced when the NASA Aura satellite ceases operations in the next year or
93 two. It will take five years or more before new satellites are launched to recover some of that lost capability. Meanwhile
94 the climate system will evolve apace with impacts on ozone recovery and air quality. Significant human-induced changes
95 in atmospheric composition may emerge from experiments referred to as Solar Radiation Management (SRM) and from
96 a projected increase in low-Earth orbit (LEO) satellite and re-entry debris.

97 The following science questions provide a focus for the work of NDACC in the coming years:

- 98 ▪ Which ozone-depleting substances, regulated by the Montreal Protocol or otherwise, will most influence the
99 ongoing stratospheric ozone recovery?
- 100 ▪ What are the processes driving atmospheric composition changes in the “Global South”?
- 101 ▪ What new stratospheric species require monitoring following atmospheric injections from volcanic eruptions
102 (e.g., Hunga Tonga) and strong wildfires?
- 103 ▪ For which atmospheric species and in which regions are enhanced measurement capabilities and precision
104 required for better trend detection and reference data?
- 105 ▪ What are the most important factors driving changes in air quality?
- 106 ▪ What are the impacts of climate change and extremes on atmospheric composition and vice versa?

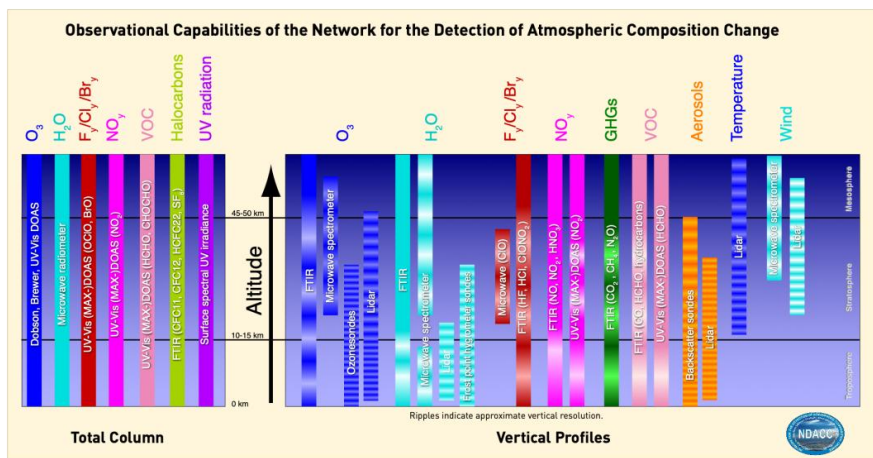
107 NDACC has succeeded for more than three decades because it has leveraged the scarce resources that support its member
108 stations as well as its archival facilities. It is exemplary in channeling technological improvements to meet changing
109 measurement and data requirements. As we enter a period of substantially reduced satellite monitoring of the upper
110 atmosphere – the “data desert” of *Salawitch et al.* (2025) – the scientific community will increasingly rely on the ground-
111 based measurements of NDACC and its Cooperating Networks to bridge data gaps or replace observational methods for
112 some atmospheric species. This challenge is compounded by the prospect of new modalities of atmospheric composition
113 change that require innovative measurement strategies.

114 This paper reviews NDACC achievements since the publication of *De Mazière et al.* (2018). These are discussed in the
115 light of the seven NDACC cardinal objectives and optimization of its strategy to best address the science questions above.
116 The paper is organized into six sections. Section 2 describes the organization of the network. Section 3 describes
117 NDACC’s partnerships and stakeholders. Section 4 summarizes NDACC’s achievements in recent years. Section 5



118 describes technical and scientific challenges facing NDACC. Section 6 looks ahead to prospects for the coming decade
119 and beyond.

120 **2 The organization of NDACC**



121
122
123 **Figure 1: Chart of NDACC observational capabilities is color-coded by observed atmospheric species and parameters with**
124 **chemical formulas listed at the top. The altitude range of profiles illustrates approximate vertical resolution associated with**
125 **each measurement technique (light horizontal stripes on vertical columns). Two horizontal dashed lines define approximate**
126 **levels of tropopause and stratopause.**

127 NDACC collects atmospheric composition data at 118 globally distributed stations with over 170 active instruments.
128 Figure 1 shows NDACC's portfolio of long-term and campaign-based measured species and parameters. These include
129 aerosol, BrO, C₂H₂, C₂H₄, C₂H₆, CCl₂F₂, CCl₃F, CH₃OH, CH₄, CH₂Cl, chlorine, ClONO₂, CO, CO₂, COF₂, H₂CO, H₂O
130 and isotopologues, HCHO, HCl, HCN, HCOOH, HF, HNO₃, HONO, N₂O, NH₃, NO, NO₂, OCIO, OCS, O₃, PAN, SF₆,
131 temperature, spectral UV irradiance, and wind. NDACC refocuses its objectives as measurement priorities evolve,
132 maintaining high data quality, quick archiving and rapid open data access in compliance with FAIR (Findable,
133 Accessible, Interoperable, and Reusable) data principles. More information about FAIR can be found at e.g. GOFAIR
134 (<https://www.go-fair.org/>).

135 Instrument Working Groups (Dobson, Brewer, FTIR, Lidar, Microwave, Sonde, UV/Vis, Spectral UV) oversee
136 instrument and algorithm quality, providing expertise and resources for teams developing new instruments interested in
137 NDACC affiliation. The Satellite Working Group fosters collaboration between NDACC and satellite missions and
138 provides meteorological data to the NDACC database via NOAA/NCEP. The Theory and Analysis Working Group
139 promotes NDACC data use and supplies model output to aid observation interpretation.

140 NDACC recognizes the value of collaboration with external measurement and analysis networks that operate
141 independently. To foster this partnership, the NDACC offers a "Cooperating Network" (CN) designation. This allows
142 for mutual data access and network representation in the annual meetings while maintaining each network's integrity.
143 Further details on agreements with Cooperating Networks appear in Section 3.



144 The NDACC Steering Committee is the organizational backbone of the network (see Fig. A1 in Appendix A, and the
145 most up-to-date version in [> ABOUT > Organizational Structure](http://www.ndacc.org)). Established in 1989, the Steering
146 Committee (SC) includes all NDACC components. In addition to the Co-Chairs, it is composed of representatives from
147 each Instrument Working Group (IWG), the Theory and Analysis Working Group, and the Satellite Working Group.
148 Each CN has representatives on the NDACC SC. The IWGs promote exchange of expertise among NDACC members
149 and the CN and support for establishing new measurement sites or new instrumentation at existing sites. Functional and
150 Ex-Officio SC positions are used for tasking and/or reviewing of specific science matters and for addressing special
151 NDACC-related issues; they ensure that international organizational interests are represented. Emeritus SC
152 Representatives also provide expertise on measurements and science, including historical perspectives on evolving
153 NDACC needs. SC member terms are finite but renewable. The list of current SC members is available on the NDACC
154 webpage (ndacc.org).
155 NDACC organizational structure (Appendix A, Fig. A1) includes the Data Host Facility (DHF) where the observational
156 and support datasets are archived and made publicly available. The NDACC website provides an easy interface to the
157 DHF and promotes news and information about the network.
158 The procedures and data quality requirements for affiliating instruments with NDACC are defined in dedicated NDACC
159 Protocols that specify expectations for existing NDACC instrument types and for proposing new techniques. Other
160 protocols stipulate NDACC structure and operating procedures. All protocols are regularly updated to maintain best
161 practices.

162 **3 NDACC partners and stakeholders**

163 Since its inception, NDACC has been endorsed by international agencies and other stakeholders, including United
164 Nations Environment Program (UNEP), the International Ozone Commission (IO3C) of International Association of
165 Meteorology and Atmospheric Sciences (IAMAS) and the Global Atmosphere Watch (GAW) Program of the World
166 Meteorological Organization (WMO). The current landscape of NDACC stakeholders is presented in Fig. 2, grouped in
167 categories: global watch programs, scientific assessments and research programs, cooperating networks, satellite
168 programs, research partners and infrastructures, and operational services. Exchanges with the stakeholders occur through
169 their SC delegates and reciprocally through the participation of NDACC delegates in stakeholder committees or creation
170 of formal agreements.



171

172 **Figure 2. Overview of NDACC stakeholders.**

173 **3.1 Engagement with international environmental programs**

174 NDACC data are essential to the global atmosphere watch program data centers operated under the auspices of the WMO,
175 UNEP and the UN Framework Convention on Climate Change (UNFCCC). NDACC contributes most of the atmospheric
176 composition Essential Climate Variables (ECVs) required by GCOS (Global Climate Observing System) and play an
177 essential role in WMO's Global Greenhouse Gas Watch (GGGW) approved in May 2023. NDACC delegates serve on
178 several GAW Expert Groups and participate in WMO's Rolling Review of Requirements process in support of the WMO
179 Integrated Global Observing System (WIGOS). Its responsibilities as a Contributing Network to GAW were laid out in
180 a formal agreement between both Parties in 2022.

181 **3.2 Engagement with scientific assessments and research programs**

182 NDACC is a major contributor to the following assessments: the quadrennial WMO/UNEP Scientific Assessment of
183 Ozone Depletion; the Tropospheric Ozone Assessment Reports (TOAR-II) under the umbrella of International Global
184 Atmospheric Chemistry (IGAC); Intergovernmental Panel on Climate Change (IPCC) assessments. NDACC also
185 contributes to research programs aimed at understanding links among changes in atmospheric composition, dynamics
186 and transport, and the evolution of air quality and climate. Joint activities include the Atmospheric Processes And
187 their Role in Climate (APARC, formerly known as Stratospheric Processes And their Role in Climate, SPARC) and
188 Global Energy and Water Exchanges (GEWEX) projects sponsored by the World Climate Research Program. The
189 Long-term Ozone Trends and Uncertainties in the Stratosphere (LOTUS-1 and -2) and Observed Composition Trends
190 And Variability in the Upper Troposphere and Lower Stratosphere (OCTAV-UTLS) projects rely on NDACC
191 observations to assess ozone and atmospheric composition trends and their uncertainties. NDACC data serve as a



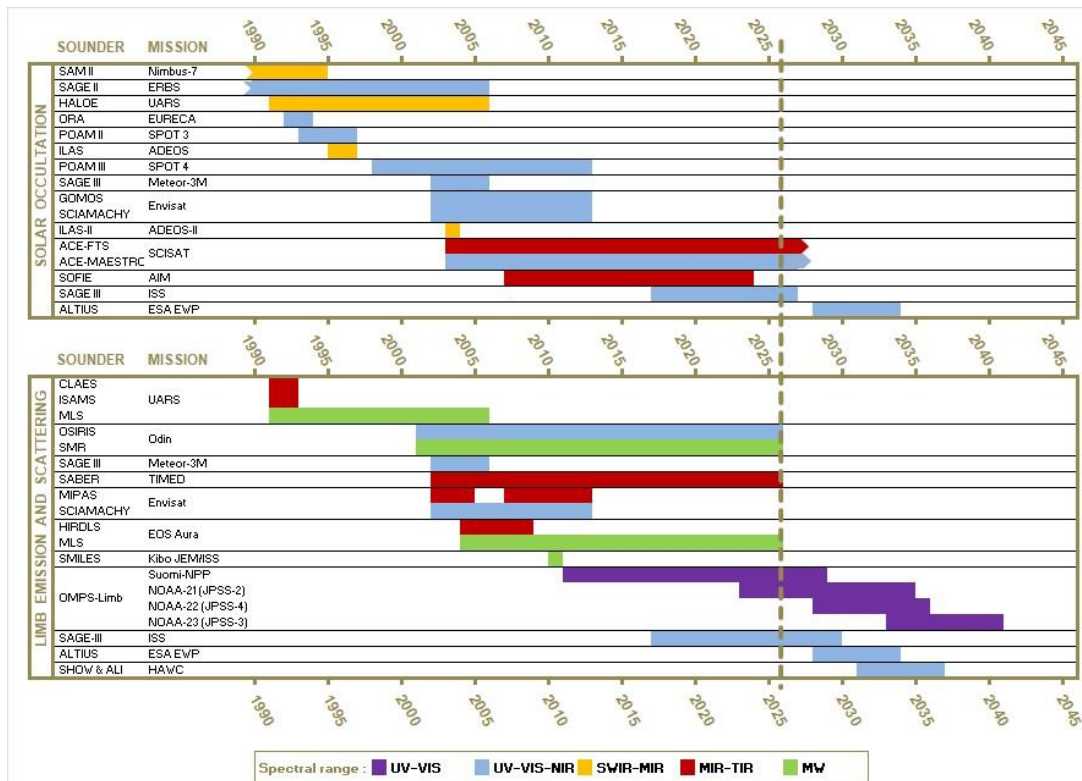
192 reference for climate model development and evaluation in the WCRP core project Earth System Modelling and
193 Observations (ESMO).

194 **3.3 Engagement with Cooperating Networks, research partners and infrastructures and operational services**

195 To widen its scope and foster collaboration on complementary measurements, NDACC has long had agreements with
196 Cooperating Networks (CN, see Figure 2). CN agreements since 2018 have been established with the European Brewer
197 Network (EUBREWNET), the Pandonia Global Network (PGN), and the Tropospheric Ozone Lidar Network (TOLNet).
198 The European Research Infrastructure for Aerosols, Clouds and Trace Gases (ACTRIS), established as a European
199 Research Infrastructure Consortium in 2023 (Laj et al., 2024) supports and shares scientific objectives and user
200 communities with NDACC. To avoid discrepancies among instrument, measurement, and data protocols related to
201 common products, a Memorandum of Understanding between NDACC and ACTRIS defines how the Parties operate to
202 maximize benefits to users through exchange of data and expertise. For example, the ACTRIS Centre for Reactive Trace
203 Gases Remote Sensing (CREGARS) will serve the NDACC community through the maintenance of central data
204 processing units (Section 4.4.2), and the provision of training and consultancy for compliance with ACTRIS/NDACC
205 requirements; the ACTRIS Data Portal (formerly GEOnet data portal) is a gateway to complementary data and services.
206 Agreements with the Copernicus Atmosphere Monitoring Service (CAMS) facilitate the use of NDACC reference data
207 for independent evaluation of CAMS global and regional data products and reanalysis, and with the Copernicus Climate
208 Change Service to deliver NDACC Climate Data Records of ECVs to the Climate Data Store (CDS). Whereas the
209 NDACC Protocol for Data Providers requires consolidated data archiving in the DHF for public availability within one
210 year after acquisition, a majority of NDACC PIs have moved to faster delivery of controlled quality data, for example,
211 meeting timeliness and quality requirements specific to CAMS Rapid Delivery.

212 **3.4 Engagement with satellite observations**

213 A primary objective of NDACC has always been providing reference measurements to support geophysical validation
214 and evolution of satellite atmospheric composition products. The network helps validate various phases of satellite data
215 reprocessing from a vast array of atmospheric composition missions to date as shown in Fig. 3 (limb) and Fig. 4 (nadir).

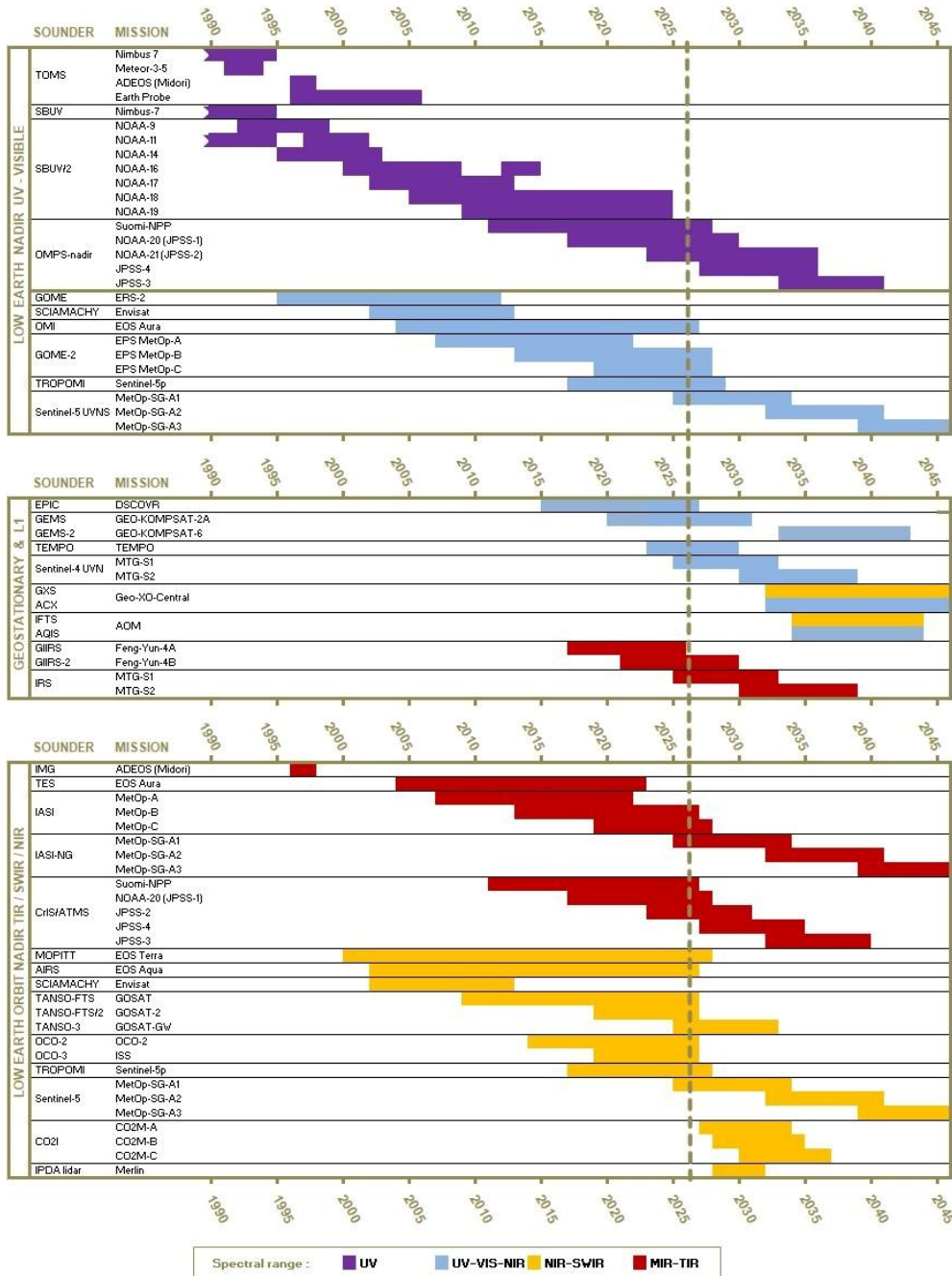


216

217

218 **Figure 3. Timelines for limb solar occultation (upper panel) and limb emission (lower panel) satellite sensors that have been,
 219 are, or will be supported by NDACC observations.**

220





225 Several space agencies are represented on the NDACC Steering Committee and Satellite Working Group (WG). A strong
226 level of cooperation between NDACC and space agencies at the level of Fiducial Reference Measurements (FRM) has
227 improved NDACC's response to ever more stringent satellite validation requirements for data quality, traceability,
228 uncertainty assessment, cross-network harmonization and timeliness of data access (Goryl et al., 2023). Close links exist
229 with the European Satellite Agency (ESA) Validation Data Centre (EVDC) hosted at the Norwegian Institute for Air
230 Research (NILU) and with NASA's Aura Validation Data Center (AVDC) which both mirror NDACC data.
231 At the inter-agency level, NDACC is represented on the Atmospheric Composition Sub Group of the Working Group on
232 Calibration and Validation (WGCV) of the Committee on Earth Observation Satellites (CEOS), an intergovernmental
233 organization ensuring international coordination of civil space-based Earth observation programs and promoting
234 exchange of data to optimize societal benefit.
235 In recent years, NDACC has made significant progress towards the FAIRness of its data. As a result, NDACC serves as
236 a reference to assess the mutual consistency of the satellites implemented in constellations by the CEOS Atmospheric
237 Composition Virtual Constellation (AC-VC) for air quality, for greenhouse gases and for ozone. NDACC also maintains
238 up-to-date content in validation protocols and guideline documents, and in strategic planning documents defining needs,
239 roadmaps, and frameworks for fit-for-purpose validation of the international satellite constellations for atmospheric
240 composition monitoring, such as the Quality Assurance Framework for Earth Observation (QA4EO) and FRM principles
241 and maturity matrix.
242 Operational satellites feeding numerical weather prediction and environmental services require a fast response to
243 validation needs. Several operational validation systems have been implemented in a staggered approach, product by
244 product, e.g., NOAA's Products Validation System (NPROVS) and the ESA/ Copernicus Validation Data Analysis
245 Facility (VDAF). Operational validation systems are being developed at EUMETSAT for the recently launched
246 Copernicus Sentinel-4 and -5 missions and the upcoming Anthropogenic Carbon Dioxide Monitoring constellation
247 (CO2M). While NDACC is already supporting operational programs with rapid delivery of data, it is anticipated that
248 there will be a need in the near-future to develop mechanisms for delivery of near-real-time (NRT) NDACC data on a
249 contractual basis. With the advent of operational satellite missions that – among other goals – serve to provide data to
250 inform efforts to control emissions of atmospheric pollutants, the appropriate validation protocols and associated
251 requirements for independent validation data must be developed: again, NDACC has an important role to play in this
252 evolution.

253 **4 Highlights of NDACC scientific achievements**

254 Recent achievements, described in this section, include discoveries related to both stratosphere and troposphere,
255 synergistic collaboration with satellite observations, and advances in network infrastructure. In all endeavors, NDACC's
256 temporal coverage and emphasis on standardized instruments, data-processing methods and protocols, have been
257 essential in creating the high-quality data required for quantifying chemical composition changes. Nearly 500
258 publications since 2018 attest to NDACC's scientific contribution, e.g., <https://ndacc.org/publications>. Highlights of
259 stratospheric and tropospheric research appear in Sections 4.1 and Section 4.2 respectively. Although not exhaustive, the
260 examples feature a range of scientific issues and perspectives. Section 4.3 discusses satellite collaborations and NDACC



261 contributions to validation. Section 4.4 illustrates NDACC's advances in instrumentation, technology and archiving
262 infrastructure, i.e., those capabilities and practices that make NDACC a uniquely valuable resource for the global
263 atmospheric research community.

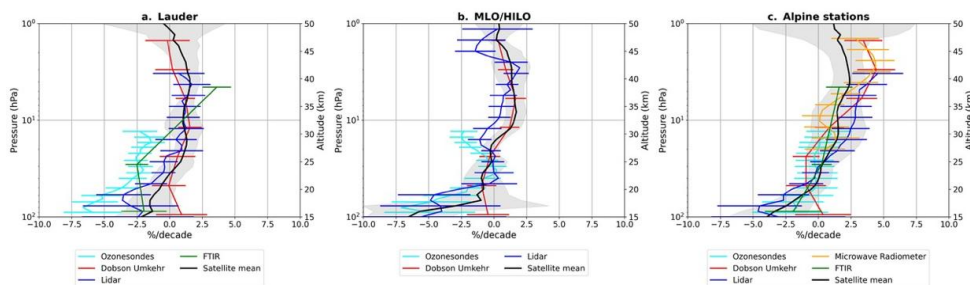
264 **4.1 NDACC stratospheric composition observations**

265 As a remote sensing network, the NDSC began with a primary focus on stratospheric composition: ozone, ozone-
266 depleting substances, and water vapor, and that commitment remains to the present.

267 **4.1.1 Stratospheric Ozone Trends.**

268 Section 3.2 described how NDACC is an integral component in SPARC/APARC research focus areas and the
269 quadrennial WMO/UNEP Scientific Assessments of Ozone Depletion. Within APARC/LOTUS, statistical multi-linear
270 regression models were used to detect linear decadal trends in the ground-based (i.e., NDACC, WMO GAW, SHADOZ)
271 and satellite ozone records (Godin-Beekmann et al., 2022) over the 2000–2020 period. The study confirmed significant
272 ozone increase in the upper stratosphere using satellite records averaged in three broad latitude bands, varying from 1.6
273 to 2.2 % per decade (Godin-Beekmann et al. 2022; 2022 WMO Ozone assessment). Fig. 5 shows longitudinally resolved
274 merged satellite records compared to ground-based data, i.e., from lidars, ozonesondes, Dobson Umkehr, microwave
275 radiometers and FTIR, that confirm the satellite trends. Non-linear behavior in the decline of lower stratospheric ozone
276 (60°S–60°N, below 24 km) during the post-2000 period was first reported by Ball et al. (2018). By applying dynamical
277 linear modeling (DLM) to the Arosa/Davos homogenized Dobson Umkehr record, Maillard Barras et al. (2022) showed
278 that upper stratospheric trends only became significantly positive after 2004, at 0.2–0.5% per year; negative trends persist
279 in the middle stratosphere and were more significant in the lower stratosphere from 2008 to 2018.

280



281

282 **Figure 5. Ozone profile trends post-2000 from selected ground-based NDACC stations: (a) Lauder, Southern Hemisphere**
283 **station, (b) tropical Mauna Loa and Hilo (ozonesonde) stations, (c) combined Alpine North Hemisphere stations. From Sofieva**
284 **et al. in review.**

285

286 APARC OCTAV-UTLS utilizes a dynamical coordinate system (i.e. tropopause, equivalent latitude, etc. derived from
287 MERRA-2 reanalyses) for binning the high-resolution ozone records to separate transport, chemical, and mixing
288 processes in the UTLS region. The method was implemented using several NDACC ozonesonde and lidar high-resolution
289 profiles, aircraft (Civil Aircraft for the Regular Investigation of the atmosphere Based on an Instrument Container) and
290 satellite (Aura/MLS and ACE-FTS) observing systems (Millan et al., 2023). The result is reduced sampling bias among



291 records, with ground-based and satellite data both revealing patterns of changing atmospheric dynamics (Millan et al,
292 2024) and a reduction of uncertainties in fitted trends (Millan et al, 2025).

293 Investigation of the Arctic stratospheric ozone depletion during an unusually strong and stable polar vortex in 2019/2020
294 winter (Bognar et a. 2020) relied on long-term observations by NDACC UV-VIS, FTIR, ozonesondes and Brewer
295 instruments located at the Polar Environment Atmospheric Research Laboratory in Eureka, Canada (80°N, 86°W).
296 Cooperating network observations (PGN, Système D'Analyse par Observations Zénithales or SAOZ), non-NDACC lidar
297 and the SLIMCAT model simulations were used to quantify ozone loss. The paper highlighted the importance of
298 combining NDACC measurements with models for attribution of ozone loss processes for predicting ozone recovery.

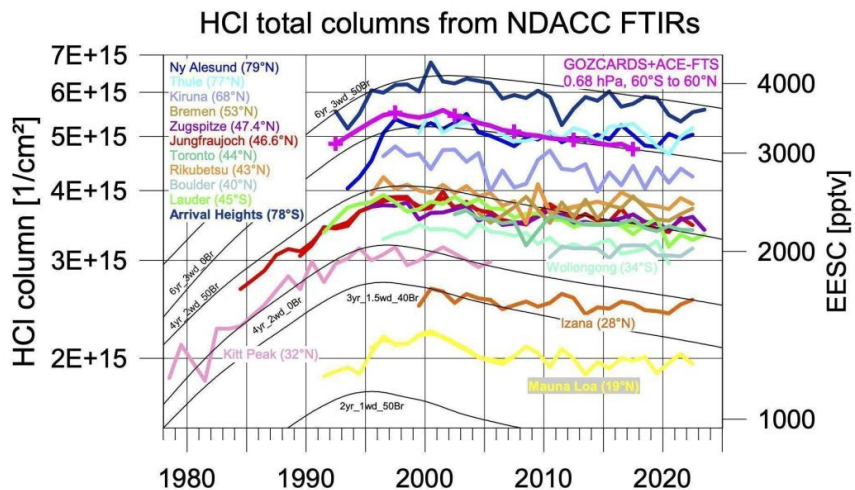
299 **4.1.2 Ozone-depleting substances, halogenated stratospheric reservoir species and stratospheric circulation**

300 NDACC data were crucial in detecting the unexpected slow decrease of CCl_4 , forcing a re-evaluation of missing sources,
301 sinks and atmospheric lifetime (SPARC, 2016; Chipperfield et al., 2016). NDACC data confirmed the unexpected
302 emissions of CFC-11 (CCl_3F) after 2012 (Montzka et. al., 2018, Chipperfield et al., 2021, Pardo-Campos et al., 2022),
303 which resulted in a slowing of its atmospheric decay, potentially delaying ozone recovery.

304 In the Ozone Assessment trends in the Jungfraujoch FTIR time series of CFC-11, CFC-12, HCFC-22, HCFC-142b, CCl_4 ,
305 CF_4 and SF_6 compared well with those derived from satellite and in situ surface data (Laube et al., 2022; Chapter 1 in
306 WMO 2022). Work continues with CFC-11, CFC-12, HCFC-22 (Polyakov et. al., 2021) and HFC-23 (Takeda et. al.,
307 2021) using innovative retrieval approaches and water vapor continuum models. A study using data from 16 NDACC
308 FTIR stations quantified decreases in the growth rate of atmospheric HCFC-22 columns derived from harmonized
309 retrievals (Zhou et al, 2024).

310

311 Transport of source ODSs to the stratosphere maintains halogen reservoir species. The most abundant chlorine- and
312 fluorine-bearing reservoirs, HCl , ClONO_2 , HF , and COF_2 , are standard NDACC data products. Fig. 6 shows the evolution
313 of total column HCl from several NDACC stations and the evolution of 10°S – 60°N lower stratospheric HCl from Global
314 OZone Chemistry And Related trace gas Data records for the Stratosphere (GOZCARDS) and ACE-FTS observations.
315 Because only second-order reservoirs are missing, the weighted combination of the respective time series represent
316 budgets of stratospheric inorganic chlorine and fluorine.



317

318 **Fig. 6.** Total column HCl, the predominant reservoir of Cl, time series from a subset of the NDACC stations representing
 319 latitudes from 78°S to 79°N. Included is the aggregate satellite time series for 60°S–60°N GOZCARDS,
 320 augmented with ACE-
 321 FTS HCl and Equivalent effective stratospheric chlorine (EESC) model (solid curves represent ODS lifetime and Br efficiency,
 322 https://ozonewatch.gsfc.nasa.gov/facts/eesc_SH.html).

322 NDACC data answer questions about atmospheric change that would otherwise remain speculative. Minganti et. al.
 323 (2022) used multi-decade satellite and NDACC data to evaluate WACCM modeled N₂O trends to better understand
 324 changes in the Brewer-Dobson circulation. Strahan et al. (2020) used MLS HCl and HNO₃ data, model output from
 325 GMI (NASA's Global Modeling Initiative) and measurements from 9 globally dispersed NDACC stations to find (i) a
 326 decrease in the age of air of the southern hemisphere lower stratosphere relative to the north by about 1 month/decade
 327 and (ii) a 5-7 y variability in both HCl and HNO₃ total columns. The 1994–2018 NDACC record provided more
 328 conclusive evidence as it spans 3-plus Solar cycles (11+ years) not available in a single satellite record. The analysis
 329 generally supports the finding that the Solar cycle confounds statistical trend regression on the QBO (quasi-biennial
 330 oscillation) if not accounted for. Alternatively, N₂O records from the NDACC FTIR stations helped validate the ACE-
 331 FTS satellite hemispheric data and global model simulated changes in Brewer Dobson global circulation (Minganti et al,
 332 2021).

333 **4.1.3 Water vapor observations**

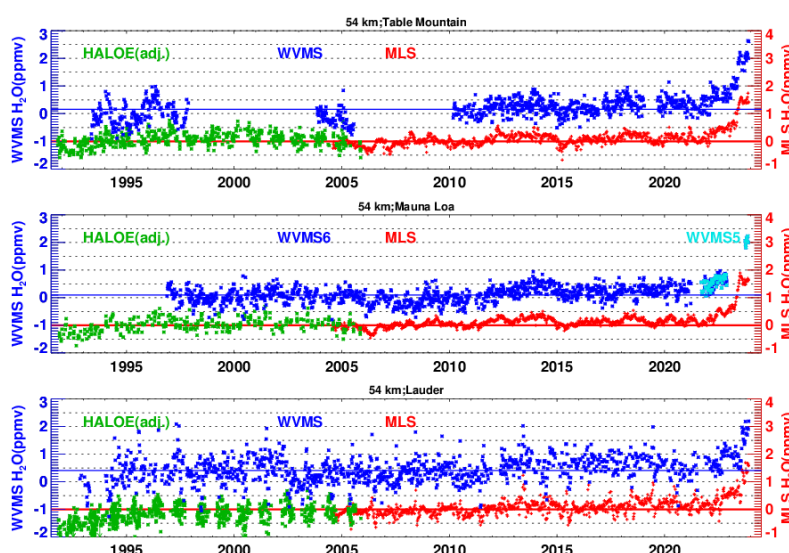
334 Detection of small water vapor trends in the upper troposphere, stratosphere and mesosphere is hampered by differences
 335 among instruments and sites, as well as natural variability in the troposphere and the large 2022 volcanic water vapor
 336 injection into the middle stratosphere. The APARC Water Vapor Assessment II intercomparison of satellite and ground-
 337 based microwave measurements, thoroughly investigated trends in water vapor between pressures of 3 hPa and 0.03 hPa
 338 (Nedoluha et al, 2017). Agreement between satellite retrievals and ground-based microwave instruments was generally
 339 within ±10%. This assessment also included an intercomparison of relative humidity from 19 limb-viewing satellites and
 340 the Vaisala RS92 radiosonde coincident with frost point instruments from NDACC (and other) sites between pressures



341 of 300-100 hPa (Read et al., 2022). Agreement of relative humidity in the upper troposphere measured by space-based
342 and frost-point instruments was on average within $\pm 30\%$, with an additional 30% variability; the Vaisala R92 radiosonde
343 was not recommended for use at pressures below 200 hPa.

344 **4.1.4 Hunga volcanic eruption**

345 On 15 January 2022, the eruption of the Hunga undersea volcano at 20S injected ~ 140 - 150 Tg of water vapor (H_2O) into
346 the atmosphere (Millan et al., 2022; Nedoluha et al., 2024). The bulk of the injection was in the lower stratosphere where
347 it was measured by balloon-borne sondes (Vömel et al. 2022). Not only was the plume injection observed from NDACC
348 stations, a rapid-response team deployed to Réunion Island within one week to make sonde observations (Evan et al.,
349 2023; Asher et al., 2023; Baron et al., 2023). Water vapor from the Hunga plume moved equatorward from its original
350 injection site, where it was first measured in the mid-stratosphere by ground-based microwave instruments at the NDACC
351 station at Mauna Loa, Hawaii (19.5°N) in April 2022 (Nedoluha et al., 2023a). Fig. 7 shows water vapor anomalies at
352 54 km (just above the stratopause) measured by ground-based microwave instruments at Mauna Loa; Lauder, New
353 Zealand (45.0°S); and Table Mountain, California (34.4°N). In 2022, water vapor mixing ratios at all three sites were
354 unusually large, partly due to dynamical conditions (Nedoluha et al., 2023b). In 2023 water vapor at Table Mountain and
355 Mauna Loa was significantly higher than ever observed in 30+ years of measurements at these (Nedoluha et al., 2024).
356 Lauder showed record-breaking mixing ratios, but short-term weekly anomalies of similar magnitudes can occur during
357 certain seasons due to dynamical variations. Finally, in late 2023/early 2024, ~ 2 years after the eruption, maximum water
358 vapor anomalies were observed at all three sites at 54 km. These findings are described in more detail in the APARC
359 “The Hunga Volcanic Eruption Atmospheric Impacts Report” (APARC, 2025).
360



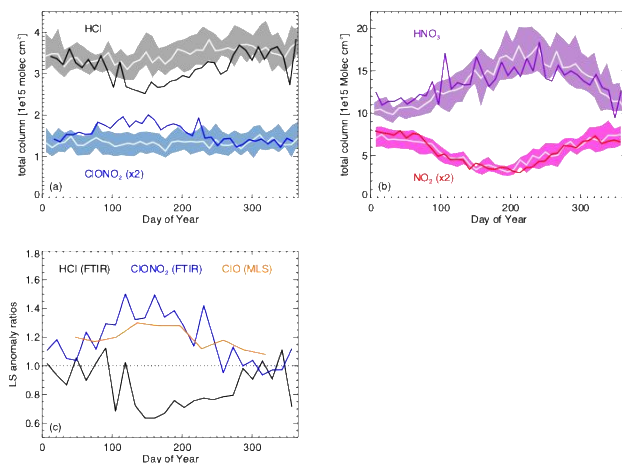
361
362 **Figure 7.** Water vapor volume mixing ratio anomalies at 54 km from \sim weekly ground-based microwave measurements at
363 Table Mountain, California (34.4°N , 242.3°E), Mauna Loa, Hawaii (19.5°N , 204.4°E) and Lauder, New Zealand (45.04°S ,
364 169.68°E). The anomaly is calculated relative to a climatology based on Aura MLS measurements from 2004-2021. From
365 Nedoluha et al. (2024).



366 **4.1.5 Extreme Australian wildfires and stratospheric chemistry**

367 In late December 2019 and early January 2020, Australian New Year wildfires injected record-breaking amounts of
368 smoke and aerosol into the southern hemisphere stratosphere. Aerosols were injected up to 32 km, resulting in a bimodal
369 size distribution as was observed in sonde flights launched at Lauder, New Zealand (Asher et al., 2024). Although
370 heterogeneous reactions on stratospheric aerosol surfaces have been known since early analyses of the Antarctic ozone
371 hole, less was known about reactions on black or brown carbon from biomass burning smoke. What NDACC and satellite
372 observations revealed in the post-fire months was unprecedented stratospheric chlorine partitioning (Fig. 8; Strahan et
373 al., 2022) which has important implications for predicting stratospheric ozone in a more wild-fire prone world. Satellite
374 observations of fire-perturbed HCl, ClONO₂, HF, O₃, N₂O and NO₂ by NDACC and H₂O, ClO and aerosol extinction
375 were reported by Santee et al. (2022) and Boone et al. (2020). Chemical simulations by Solomon et al. (2023) proposed
376 that chlorine partitioning was caused by oxidized organics and sulfates increasing hydrochloric acid solubility (and
377 associated heterogeneous reaction rates. This is supported by the observed enhanced ClONO₂ and decreased HCl,
378 although Strahan et al. (2022) pointed out that definitive ozone loss is not confirmed due to entangled chemistry/transport
379 effects. Ozone losses appear to peak in May-June.

380



381

382 **Figure 8. (a) 2020 9-day average of Lauder FTIR total column HCl and ClONO₂ (scaled for clarity) along with associated**
383 **2010-2019 mean (white) and 1 standard deviation (shaded). (b) Same as (a) but for HNO₃ and NO₂ (scaled for clarity). (c)**
384 **Lower stratosphere column (LS, ~150-50 hPa, ~12-21 km) 2020 anomalies (9-day average, ratioed to 10-year means, 2009-**
385 **2019) for HCl and ClO. Total column ClONO₂ anomalies are displayed because there is insufficient signal for a ClONO₂ LS**
386 **column. Aura-MLS ClO observations are averaged over 40°-50°S. (after Strahan et al. 2022)**

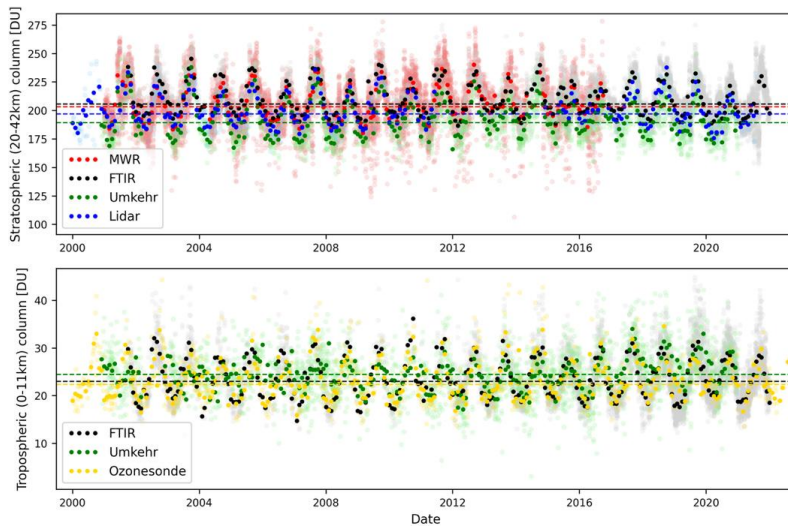
387 **4.2 NDACC tropospheric composition observations**

388 NDACC research in the 2000's has focused increasingly on tropospheric composition and radiation as described
389 below.



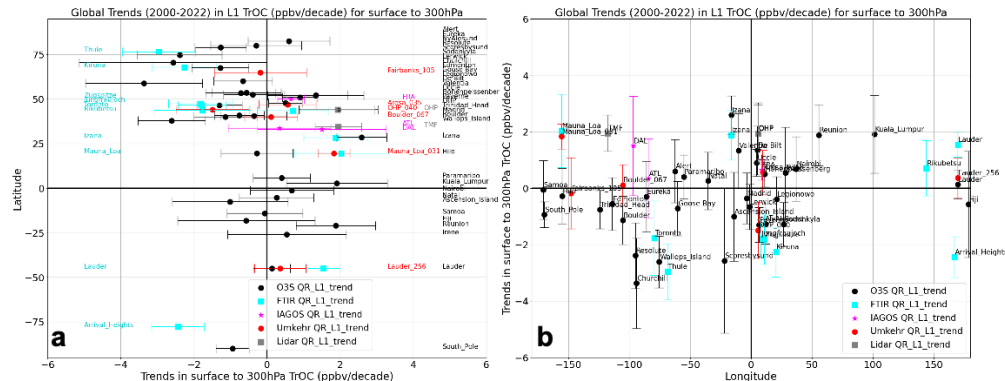
390 **4.2.1 NDACC and the Tropospheric Ozone Assessment Report (TOAR)**

391 NDACC played a major role in analyzing global tropospheric ozone trends in the second phase of IGAC's Tropospheric
392 Ozone Assessment Report (TOAR II; see TOAR I reports by Gaudel et al., 2018; Tarasick et al. 2019). Within the
393 HEGIFTOM working group (Harmonization and Evaluation of Ground-based Instruments for Free-Tropospheric Ozone
394 Measurements), records from NDACC and affiliated networks for four instruments – FTIR, Lidar, Brewer/Dobson
395 Umkehr, ozonesonde – were reprocessed with absolute reference standards and archived to produce ozone column data
396 with uniform formats with uncertainty estimates and quality flags (Van Malderen et al, 2025a). Fig. 9 shows an
397 intercomparison study at the multi-instrumented Lauder supersite (Björklund et. al., 2024) for both stratospheric and
398 tropospheric columns based on time-series for 2000-2022. More than 50 articles from TOAR II analyses, including those
399 based on HEGIFTOM and other ground-based data, with satellite products, have been published in a TOAR II special
400 collection (see https://bg.copernicus.org/articles/special_issue10_1256.html).



401
402 **Figure 9. Upper:** Time series (2000-2022) ozone columns (20-42 km) in Dobson Units (DU) from four remote sensing techniques
403 at Lauder, New Zealand. Shaded points are all data, highlighted points are monthly means, dashed lines are median of all data
404 by technique. Lower panel shows the tropospheric ozone column (defined as surface to 11km). After Björklund et al., (2024).

405 Trends for individual station HEGIFTOM/NDACC ozone columns, augmented by landing/takeoff profiles from the In-
406 service Aircraft for a Global Observing System (IAGOS) airports, were calculated following TOAR-II guidelines on
407 metrics, units, time range, and statistical trend model in a series of studies (e.g., Van Malderen et al., 2025a,b; Gaudel et
408 al., 2024; Thompson et al., 2025). A summary of median trends for a tropospheric total column (TrOC, specified as
409 surface to 300 hPa, for 2000 to 2022, based on the HEGIFTOM data, appear in Fig. 10. Trends are illustrated with 2σ
410 uncertainties for 55 sites (Van Malderen et al., 2025a) as a function of latitude (Fig. 10, left) and longitude (Fig. 10,
411 right). The HEGIFTOM-derived trends mark a turning point for the tropospheric ozone community. Having ground-
412 based ozone trends as a definitive reference for still-evolving satellite products, some covering < 10 years, is essential
413 for rigorous evaluation of ozone trends based on satellite data (Hubert et al., TOAR-II Satellite Ozone Report, 2025).



414

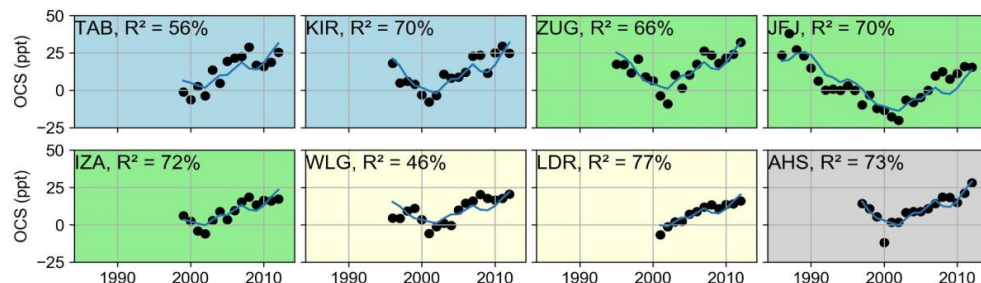
415 **Figure 10.** Tropospheric column ozone (TrOC, surface to 300 hPa) trends in ppbv/decade, determined from three IAGOS
416 airport and four NDACC instruments: ozonesondes, FTIR, Umkehr, and Lidar. Calculation was made using all data (L1, 2000
417 to 2022) by Quantile Regression. Uncertainties at $\pm 2\sigma$. Most stations exhibit median trends within ± 3 ppbv/decade (Van
418 Malderen et al., 2025a). a) trends as function of latitude, b) trends as function of longitude.

419

4.2.2 Long-term trends in whole atmosphere carbonyl sulfide.

420
421
422
423
424
425
426

Carbonyl sulfide (OCS), the reservoir sulfur species in the free troposphere, is a product of anthropogenic, biogenic and oceanic emissions and the largest source of sulfur transported to the stratosphere during periods of low volcanic emissions, helping maintain the lower stratospheric sulfate aerosol layer. Despite these important roles, it remains under-observed. NDACC FTIR OCS measurements are unique in having near-global coverage for 3+ decades. Hannigan et al. (2022) derived trends in the lower free troposphere and the lower stratosphere, showing distinct trends over discrete time periods since 1986. Regression models and available proxies of varying time periods, attribute the varying trends in Fig. 11 are due primarily to anthropogenic emissions.



427

428

429
430
431

Figure 11. Fit of the annual anthropogenic emissions inventory from Zumkehr et al. (2018) to annually averaged FTIR OCS data from stations with the longest running data records. The emissions inventory is interpolated to the station location. From Hannigan et al. (2022).

432

4.2.3 Surface UV radiation: Monitoring, impacts, and research

433
434
435
436

Surface UV radiation is a crucial indicator of atmospheric change, capturing the combined effects of aerosols, clouds, ozone, and dynamics. Its reach extends to public health, impacts on terrestrial and aquatic ecosystems and the degradation of materials like plastics into microplastics. Regular high-precision NDACC spectral UV observations are conducted at 12 globally distributed stations, strategically located to cover diverse environments (polar, mid-latitude, tropical) to



437 ensure data collection across Earth's UV regimes. In Antarctica, continuous monitoring since 1990 has shown a slight
438 decline in overall UV exposure since the early 2000s (Bernhard & Stierle, 2020), consistent with ozone layer recovery.
439 However, ground-based measurements still record extremely high UV levels like persistent ozone holes (Cordero et al.,
440 2022). These observations have greatly advanced our knowledge of public health impacts from spatial and temporal
441 variability in UV doses (Brogniez et al., 2021). Cumulative, low-dose UV exposure has significant health implications,
442 leading to advocacy for a more nuanced understanding of UV benefits and risks (McKenzie & Lucas, 2018; McKenzie
443 et al., 2022).

444 **4.3 Satellite validation and collaboration**

445 There is considerable synergy between NDACC, with its focus on remote sensing measurements, and the satellite
446 observations community for initial validation of new space-based instrumentation, detection of long-term drifts, and
447 collaborative research. Selected highlights follow. More examples with publications appear in Appendix C, Table C1.

448 **4.3.1 Detection and quantification of long-term satellite drifts**

449 Without long-term ground-based observations, detection of drifts or steps in satellite data record is difficult. The
450 MOPITT instrument aboard NASA's EOS-Terra satellite launched in 2000 measuring near-global CO has exceeded
451 initial specifications. Buchholz et. al. (2017) used data from 14 latitudinally distributed NDACC FTIR stations to
452 determine drifts over the first 17 years. Co-located data carefully matched using the vertical sensitivity (averaging
453 kernels) to account for the respective response of each FTIR examined three MOPITT retrieval schemes. Mean bias for
454 all sites was determined to be 2.4 % for TIR-only, 5.1 % for TIR–NIR, and 6.5 % for NIR-only. The MOPITT long-term
455 bias drift is calculated to be within $\pm 0.5\% \text{ yr}^{-1}$. Aura MLS has also operated past its programmed lifetime. NDACC
456 water vapor sonde data at Lauder, Hilo and Boulder were used to evaluate, determine and correct for drifts over 15 years,
457 2005 to 2020 (Livesey et. al., 2021).

458 Stability of ground-based records themselves can be compromised by instrumental artifacts, e.g. "drop-off" in
459 ozonesonde records due to manufacturing changes (Stauffer et al., 2020), which are often detected through calibration
460 and multi-instrument intercomparison activities (Thompson et al., 2019) and by adherence to NDACC observational
461 protocols. Processing satellite and ground-based (GB) data by identical statistical methods minimizes biases in trend
462 detection while illustrating potential inconsistencies among records (Petrovavlovskikh et al., 2024).

463 Over the past 25 years, members of the NDACC ozonesonde community have been part of the WMO/GAW ASOPOS
464 (Assessment of Standard Operating Procedures for Ozonesondes) activity to optimize sonde data quality through
465 specification of standard operating procedures (SOP) including data (Smit et al., 2024). Roughly half of the 60 global
466 sonde stations have reprocessed their records. For ozonesonde data since mid-2004, satellite measurements are used to
467 evaluate the sonde profiles as shown in Fig. 12. Total column and stratospheric ozone from the sondes were compared
468 to overpass readings from satellite (Aura OMI and MLS, S-NPP OMPS, GOME-2A and -2B) from mid-2004 through
469 2021 to determine stability in the sonde measurements. Overall, the ozonesonde data show remarkable agreement
470 compared to satellite instruments. Total column ozone derived from the sondes is on average within $\pm 2\%$ of the Aura
471 OMI over the last 18+ years (Fig. 12), and the ozone profiles match Aura MLS to within $\pm 5\%$ in the mid-stratosphere up
472 to 10 hPa (Stauffer et al., 2022). The excellent agreement is achieved even with a known instrumental bias at several



473 stations (Stauffer et al., 2020). These comparisons underscore the success of the ozonesonde data reprocessing and
474 homogenization effort (Smit et al., 2021). In the 1990s, ozonesonde data uncertainty was on the order of 20%, and biases
475 near 10% in total column ozone were common. Today, data uncertainties approach 5%, with total column ozone biases
476 < 2%.

477

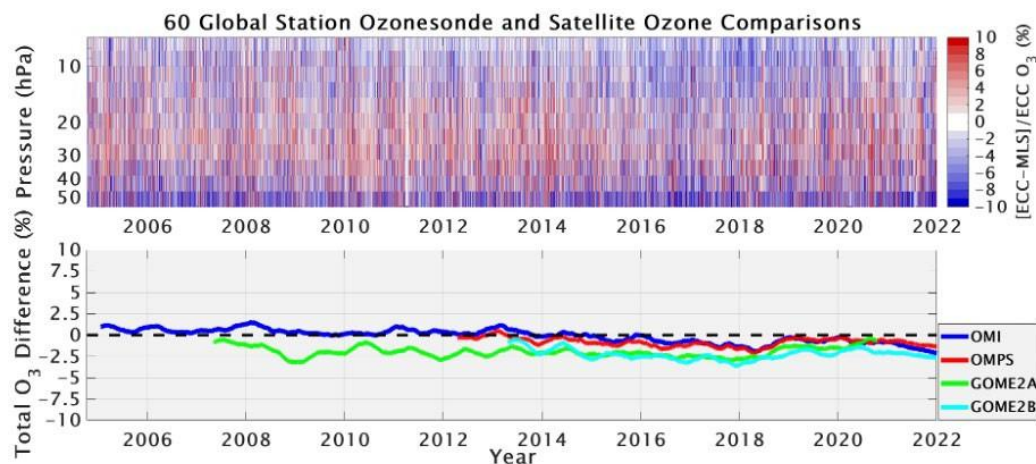


Figure 12. Coincident ozonesonde and satellite comparisons (% difference) for 60 global ozonesonde stations. (Top) Time series comparisons among all ozonesonde and Aura Microwave Limb Sounder (MLS) O₃ profiles ([ECC-MLS/ECC]) where ECC signifies the sonde value. Red (blue) colors indicate where the sonde ozone is greater (less) than MLS. (Bottom) Ozonesonde and satellite total ozone comparisons in % difference ([ECC-satellite]/ECC) for OMI (blue), S-NPP OMPS (red), GOME-2A (green), GOME-2B (cyan).

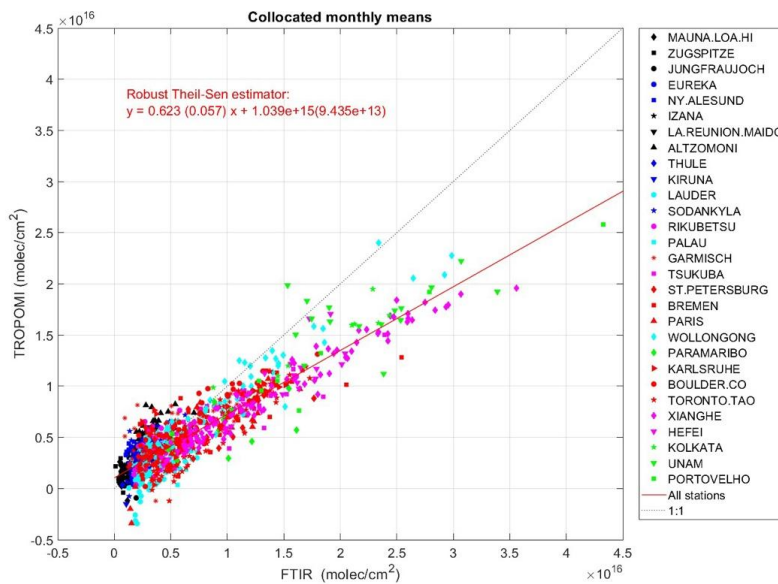
478 **4.3.2 Operational validation of HCHO and NO₂ for Sentinel-5P**

479 The operational validation service of Sentinel-5P TROPOMI relies on the fast delivery of correlative measurements
480 acquired by most of the NDACC sub-networks and several cooperating networks. Total and tropospheric ozone column
481 and profile data products are quality assessed by an operational validation server (<https://mpc-vdaf.tropomi.eu>) using
482 Brewer, Dobson, FTIR, lidar, ozonesonde and Zenith-Sky DOAS measurements acquired from pole to pole and under a
483 variety of measurement conditions and influencing parameters (Garane et al., 2019; Hubert et al., 2021; Keppens et al.,
484 2024).

485 The quality assessment of NO₂ total and partial columns relies on a holistic approach combining validation of TROPOMI
486 stratospheric NO₂ with respect to NDACC Zenith-Sky DOAS columns, tropospheric NO₂ with respect to MAX-DOAS
487 columns, total NO₂ with respect to PGN total columns (Verhoelst et al., 2021) and cloud parameters validation using the
488 ACTRIS-Cloudnet network of lidars and radars (Compernolle et al., 2021). Harmonization of NDACC FTIR NO₂
489 (Vigouroux et al., 2025), provides a new global dataset for TROPOMI validation (see S5P Quarterly Validation Reports
490 at <https://mpc-vdaf.tropomi.eu>). Stratospheric NO₂ columns measured by NDACC FTIR, Zenith-Sky DOAS and PGN
491 at pristine stations (i.e., without tropospheric NO₂ pollution) give mutually consistent validation results, showing e.g. a
492 similar station-to-station 1-sigma scatter of the bias with TROPOMI of ~5%.



493 Although not a standard NDACC product, harmonized HCHO FTIR data were produced by the network (Vigouroux et
494 al., 2018) and used for the first TROPOMI HCHO validation (Vigouroux et al. 2020). TROPOMI HCHO products were
495 shown to be biased high over clean regions by ~26% but underestimated by ~31% in polluted conditions. The robust
496 linear relationship between TROPOMI and NDACC data is shown in Fig. 13 across a range of HCHO concentrations.
497 These data are used in inverse modeling studies to correct TROPOMI and OMI products before inverting them (Oomen
498 et al., 2024; Müller et al., 2024). The high internal consistency of FTIR-based HCHO is illustrated; HCHO is now
499 archived as a standard NDACC species. The HCHO FTIR data set has been employed in other satellite validation (Lee
500 et al., 2024; Kwon et al., 2023; Ayazpour et al., 2025; Müller et al., 2024) and for characterizing errors in satellite-based
501 HCHO/NO₂ ratios (Souri et al., 2023) and for TEMPO validation over North America.



502
503 **Figure 13. Scatter plot of NDACC FTIR and TROPOMI HCHO data, after Vigouroux et al. (2020).**

504 Similarly, harmonization of NDACC FTIR NO₂ (Vigouroux et al., 2025), provides a global network dataset for
505 TROPOMI validation (Quarterly Reports at <https://mpc-vdaf.tropomi.eu>). The NDACC FTIR and Zenith-Sky DOAS
506 NO₂ columns are characterized by excellent internal consistency, showing a similar station-to-station 1-sigma scatter of
507 biases with TROPOMI of ~5% (Verhoelst et al., 2021).

508 4.3.3 Correlative observations of new species

509 Some of the most exciting advances in satellite observations are due to advances in retrieval algorithms providing data
510 products for new species. Species like methanol, ethane, ethene, ethyne and isoprene (CH₃OH, C₂H₆, C₂H₂, C₂H₄, C₅H₈
511 respectively) have been observed with the Cross-track Infrared Sounder (CrIS) (Wells et al., 2022, Wells et al., 2024,
512 Brewer et al., 2024). These species, primarily originating from biogenic and anthropogenic sources, are important as
513 ozone precursors, traceable to emissions sources. NDACC has developed new retrievals for these species, in some cases
514 providing the only validation data. The Infrared Atmospheric Sounding Interferometer (IASI) has produced a formic acid



515 (HCOOH) data product that Franco et al. (2020) validated with global NDACC FTIR data. Other new species observed
516 by NDACC are PAN ($\text{CH}_3\text{C}(\text{O})\text{O}_2\text{NO}_2$) (Mahieu et. al., 2021, Wizenberg et. al., 2022) and ammonia (NH_3) (Dammers
517 et al, 2015; Lutsch et. al., 2019, Yamanouchi et. al., 2021, Herrera et. al., 2022). See Table A1 (Appendix B) for the list
518 of species validated by NDACC observations.

519 **4.4 Advances in instrumentation, data processing and archiving infrastructure**

520 Since its inception, the NDACC mission has been to observe the atmosphere with the precision and accuracy required to
521 answer the key science questions of the day, hence the focus on state-of-the-art, calibrated, certified instrumentation.
522 Instrumentation techniques, data acquisition, and signal-to-noise specifications have greatly improved over the last three
523 decades while data processing and analysis techniques have evolved to deliver larger, better characterized, versioned
524 datasets with improved uncertainty budgets. These complex and versatile datasets are used by a more diverse research
525 community. Simultaneously, the geographical, temporal, representativeness, precision requirements of the research and
526 monitoring communities have increased. Some examples of how NDACC has responded to this new environment follow.

527 **4.4.1 Instrumental: Automation, compactness, mobility**

528 The Jet Propulsion Laboratory (JPL) Atmospheric Lidar Team has developed a compact, more affordable class of
529 tropospheric ozone differential absorption lidar (DIAL) systems. The Small Mobile Ozone Lidar (SMOL) is compact
530 enough to be readily deployed for rapid air quality measurement campaigns at 10 to 50% the cost of most existing
531 tropospheric ozone lidars (Choza et al., 2025). In June-August 2023 JPL deployed two SMOL instruments in the Los
532 Angeles Basin to participate in the NOAA-led AEROMMA-2023 campaign and in the NASA-led STAQS Mission for
533 the validation of TEMPO. By June 2024, two more SMOL instruments had been built, enabling unprecedented
534 deployment configurations for field campaigns, e.g., within a tight spatial grid for air quality studies, or at a larger,
535 synoptic scale to study long-range transport and stratospheric intrusions.

536 In 2024, a version optimized for stratospheric ozone (SMOL-X) was designed and successfully tested. SMOL-X can
537 measure vertical profiles of ozone between 5 km and 35 km altitude with a precision better than 10% for a 3-hour
538 averaging time. Because of its affordability and ease of deployment, this new class of stratospheric ozone DIAL provides
539 opportunities for NDACC deployment in remote areas, such as Antarctica, the Arctic, Asian or Africa providing the
540 opportunity to fill critical measurement gaps. NDACC continues to evaluate new measurement techniques and target
541 variables. For example, in 2020, the UV-VIS Working Group updated the instrument and validation protocols for
542 including MAX-DOAS-type instruments, several of which have been NDACC-certified since then. Wind lidar joins
543 microwave wind instruments to extend NDACC's meteorological observational capability. The Steering Committee is
544 also evaluating the addition of temperature data measured by microwave instruments.

545 **4.4.2 Migration towards central processing**

546 NDACC ensures a high standard of data quality as well as a high degree of homogenization and consistency across
547 instruments and platforms. Centralized data processing with network-wide scrutiny is a powerful tool to achieve quality,
548 consistency, and homogenization.



549 The NDACC Lidar Working Group recently built its initial centralized lidar data processor. The Global Lidar Analysis
550 Software Suite (GLASS). Initially developed to retrieve stratospheric ozone, temperature, aerosol, tropospheric ozone,
551 and water vapor for the four JPL lidars, GLASS was soon expanded to process the raw data of more than a dozen other
552 lidar instruments contributing to NDACC, TOLNet and GRUAN (GCOS reference Upper Air Network). GLASS is used
553 to support several NDACC-contributing stations on a routine basis and also serves as a transfer standard during
554 campaigns (e.g., the SCOOP and STOIC campaigns in 2016 and 2024 respectively).

555 Within the ESA FRM4DOAS consortium, a Centralised Data Processing System (CDPS) dedicated to the retrieval of
556 tropospheric and stratospheric trace gas data products from MAX-DOAS and zenith-sky light DOAS instruments has
557 been developed (Van Roozendael et al., 2024). In its current demonstration, the FRM4DOAS system generates total
558 ozone, stratospheric NO₂ profiles, and tropospheric columns and profiles of NO₂ and HCHO from approximately 20
559 stations worldwide. Retrieval algorithms are selected through community consensus, resulting in quality-controlled data
560 products being delivered daily to the NDACC rapid delivery (RD) repository and mirrored at the ESA Validation Data
561 Centre (EVDC) to serve as Fiducial Reference Measurement (FRM) for satellite validation. Like the FTIR CDPS (see
562 below) this system is also integrated within the ACTRIS Centre for Reactive Trace Remote Sensing Central
563 Facility.

564 An FTIR CDPS has also been developed to ingest infrared spectral data from standard NDACC high-resolution, moderate
565 and low-resolution instruments to accommodate rapidly delivery for Sentinel 5P and CAMS validation systems. Key
566 features are the easy integration of additional instruments and open source. For more than a dozen FTIR instruments, the
567 system provides NDACC retrievals for selected species and the capacity for both instruments and species is increasing.
568 Processing these spectra demonstrates the advantages of the CDPS:

- 569 ▪ High level of harmonization of retrieval results e.g. uncertainty budgets, regularization
- 570 ▪ Traceability of processing: e.g. registration of retrieval strategy, spectroscopy data, ensures FAIR adherence
- 571 ▪ Responsiveness to changes, e.g. prior data, spectroscopy, algorithm, reporting and guidelines (GEOMS or
572 NDACC DOI generation),
- 573 ▪ Automated rapid delivery data to NDACC DHF or other destinations,
- 574 ▪ Decreased operational workload for instrument PI, and
- 575 ▪ Uniform quality assurance across all instruments and all data levels (L0 - L2).

576 The CDPS has created advanced visualization tools for L0, L1 and L2 data accessible to the public at (<https://actris-ftir.aeronomie.be/actrisvisualizer?view=visualize>). The system is integrated into the ACTRIS CREGARS FTIR facility
577 (<https://actris-ftir.aeronomie.be/>) and used by ACTRIS National Facilities. The ACTRIS FTIR CDPS follows NDACC
578 IRWG retrieval procedures to maintain consistency with NDACC.

581 **4.4.3 Data Handling Facility: GEOMS, versioning, licensing, DOIs**

582 Fundamental issues affecting large data archives include documentation of data, tracking of data versions and
583 reprocessing, consistency of data content when shared to multiple archives, use of formatting standards, including
584 appropriate reporting of error estimates, associated auxiliary variables and metadata, safe storage of raw data, availability



585 of data to the public, acknowledgement of data used in publication, data licensing, and durability and discoverability of
586 datasets.

587 NDACC requires assurance of long-term measurement traceability and stability; change management is critical to
588 NDACC's mission. The DHF has leveraged GEOMS metadata standard to introduce data versioning capabilities (i.e.
589 identifying data processed by distinct algorithms, data with varying integration times, data corresponding to a specific
590 publication, centrally-processed and/or in-house-processed data products).

591 NDACC data are publicly available, findable and searchable at the DHF, i.e., accessible. NDACC relies on the Digital
592 Object Identifiers (DOI) to enhance the likelihood of a dataset discovery, to promote data interoperability (i.e. through
593 metadata), and to allow data records to be cited directly (often a requirement of scientific journals). EVDC provides a
594 mechanism to publish DOIs for NDACC data providers. Restrictions or openness of use of a dataset is defined by the
595 data provider as stated in the metadata file. GEOMS and NDACC recommend Creative Commons licensing
596 (creativecommons.org) which dictates how data can be used and reused.

597 The DHF stores model output from the Global Modeling Initiative (GMI) extracted at the location of NDACC stations.
598 Extracted GMI chemical transport model (CTM) datasets are available for 1985 to 2022. Output extracted at NDACC
599 station locations is also available from a GEOS-GMI simulation simulation run in replay mode (Orbe et al., 2017) to
600 constrain the meteorology to the MERRA-2 reanalysis (Gelaro et al., 2017). GEOS-GMI utilizes the GMI chemical
601 mechanism (Duncan et al., 2007; Strahan et al., 2013; Nielsen et al., 2017) as part of the GEOS atmospheric general
602 circulation model (Molod et al., 2015). The GEOS-GMI simulation, described in Fisher et al. (2024), has higher
603 horizontal resolution than the GMI CTM simulation. The GEOS-GMI datasets are currently available for 1996 to 2022
604 and Replay datasets up to 2023 with plans to continue with years. Results from Lagrangian transport simulations using
605 the Chemical Lagrangian Model of the Stratosphere (CLaMS; e.g. Pommrich et al., 2014 and references therein), which
606 was originally developed for stratospheric ozone research, are available to NDACC researchers for joint project studies.
607 CLaMS can be used as a conceptual trajectory model, as an offline, reanalysis-driven chemistry transport model, or
608 online as part of a climate model (e.g. Charlesworth et al., 2023; Vogel et al., 2023). Various CLaMS products, such as
609 pure trajectory calculations, artificial model tracers to tag air masses (e.g. surface-origin tracers, age of air), as well as
610 upper tropospheric and stratospheric chemical trace gases, can be provided (e.g. Ploeger et al., 2021; Graßl et al., 2024;
611 Groß et al., 2025; Vogel et al., 2025).

612 Physical locations of the NDACC DHF and website are at NASA Langley Research Center (LaRC), ensuring continuity
613 of infrastructure central to the network's functioning. The recent move of the DHF from its NOAA (Maryland) home at
614 NASA LaRC (Virginia) provided an opportunity for a full redesign of the interface for both data providers and users.
615 While preserving the integrity of data quality and interfaces with partnering organizations, the data ingestion now allows
616 for interactive and programmatic upload. Tools are available for checking files prior to full archiving. The query of data
617 using the database tables is available to the public via an intuitive interface, allowing for data access with identification
618 of statistics on the data, e.g., number of files, submission dates and more.



619 **5 NDACC Challenges and opportunities**

620 The structure of NDACC and how it meets the principal goal of providing the highest quality atmospheric composition
621 data were detailed in Sections 2 and 3. Section 4 illustrates major discoveries and accomplishments focusing on NDACC
622 observations since 2018. The network is not without challenges (Section 5.1). At the same time NDACC seeks to expand
623 measurements to address emerging areas that require high-quality ground-based observations (Section 5.2).

624 **5.1 Challenges**

625 **5.1.1 Technical challenges**

626 There are two general types of challenges facing NDACC. First, there are technical challenges (Section 5.1.1.1), i.e.,
627 incorporating new instruments, maintaining reference standards and consistent calibrations, and adapting to every-
628 changing archives and formats. Second, infrastructure challenges (Section 5.1.2) include sustained funding, adapting to
629 new scientific priorities while maintaining long-term measurements, changing expectations on data availability and re-
630 posting on an ever-growing population of secondary and tertiary data platforms.

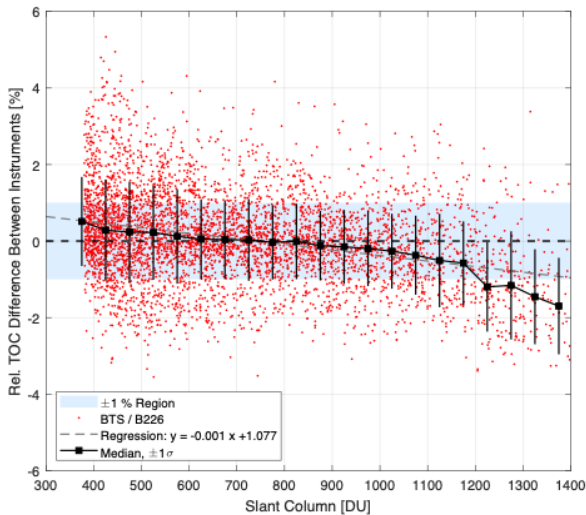
631 **5.1.1.1 Instrument and IT issues**

632 NDACC researchers often push instruments to their limits, dedicated to collecting consistently high-quality data as
633 instruments age, spare parts dwindle, the cost of maintenance increases, and some instruments are replaced with newer
634 technology.

635 Total column ozone instruments, a mainstay of satellite calibration and cross-calibration, have been deployed globally
636 for 6-7 decades. Many of the Dobson spectrophotometers used in NDACC are more than 50 years old. There are no
637 dedicated suppliers for replacement parts. Mechanical and optical properties aren't well documented. Furthermore, the
638 manufacturer of the NDACC Brewer instruments has recently discontinued production.

639 Simpler, automated and less expensive instruments have been developed, e.g., Pandora or BTS array spectrometers for
640 total ozone and UV measurements (Herman et al., 2015; Zuber et al., 2021) or moderate spectral resolution mid-IR
641 interferometers (e.g., Sha et al., 2020). Some newer instruments are still being evaluated for accuracy and multi-decade
642 stability. An example (Fig. 14) compares total ozone columns measured by a new BTS spectrometer and an NDACC
643 Brewer. When slant ozone columns are large and the sun is lower in the sky, the BTS instrument reports lower values,
644 presumably due to straylight effects that will need to be corrected.

645 Other challenges include the scarcity and/or cost of supplies, e.g., helium for launching sondes, gases used in lasers, and
646 the phase-out of certain technologies. The latter case is illustrated by the need to replace the HFC coolant (R23) in
647 frostpoint water vapor sondes. R23, a powerful greenhouse gas, is banned in accordance with the Montreal Protocol
648 Kigali Amendment.



649

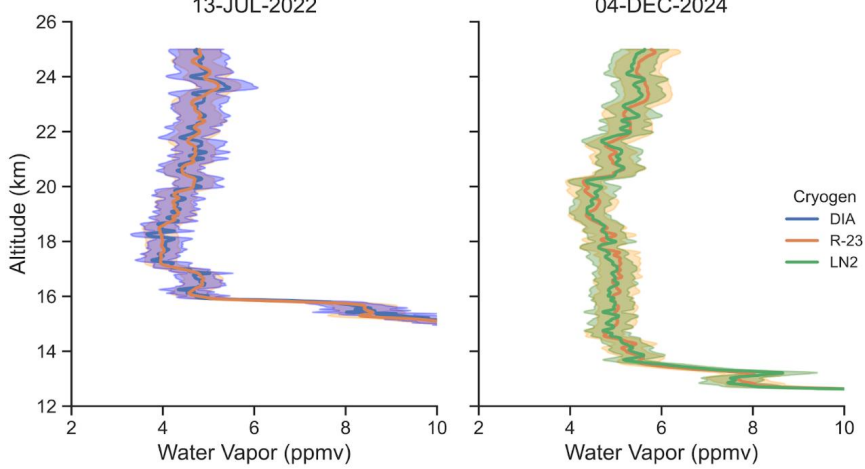
650

651

652 **Figure 14.** Relative difference between total ozone columns (TOC) measured by a modern CCD-based spectrometer (Gigahertz
 653
 654
 655

BTS) and the NDACC Brewer double-monochromator #226, shown as a function of slant TOC for observations at
 Hohenpeissenberg from November 2021 to December 2025.

Figure 15 shows profiles of water vapor from paired launches of NOAA frost point hygrometers (FPHs) using 1) dry ice
 and ethanol (DIA) and 2) liquid nitrogen (LN2). Although significant progress has been made transitioning away from
 R23, further intercomparisons with alternative cryogens are ongoing.



656

657

658

659

660

Figure 15. Near simultaneous launches from Boulder with NOAA R-23 and NOAA DIA FPHs on July 13, 2022 and with
 NOAA R-23 and NOAA LN2 FPHs on December 4, 2024. Shown are the 1-second gaussian filtered water vapor data products
 and total calculated uncertainties of each, derived using sources of error in the frost point temperature measurements and the
 reported uncertainty of the iMet-54 radiosonde pressure.

661

662

Many NDACC instruments come from small manufacturers with limited staff. This limitation makes it difficult to track
 unintentional manufacturing changes in ozonesonde production, for example, that have contributed to inconsistencies in



663 ozone profile time series (Stauffer et al., 2022). The NDACC and WMO-sponsored Assessment of Standard Operating
664 Procedures for Ozonesondes (ASOPOS) activity is standardizing procedures for ozonesonde operations and data
665 processing (WMO Report 268; Smit et al. 2024) with the idea of homogenizing long-term records using an absolute
666 ozone standard.

667 Recent problems with Raman lidar water vapor measurements illustrate an unusual challenge. Their data in regions
668 affected by UT/LS biogenic aerosols from extreme wildfires (Khaykin et al., 2020a) are contaminated by aerosol
669 fluorescence (Chouza et al., 2022). The measurements can be corrected, but with reduced signal-to-noise ratio,
670 compromising reliable trend detection. Raman lidar observations performed at 532 nm are an alternative.

671 Ongoing changes in IT, lasers, spectrometric systems, components, etc., across 40 years or more is a challenge that
672 requires expertise and costly efforts to digitize historic data and to upgrade to new systems. To guarantee trend-worthy
673 data, parallel operation of old and new systems, sometimes over years, is essential and required by NDACC protocols.
674 Remote access to and /or automatic operation of instruments is increasingly available. This reduces staffing requirements
675 and cost, although in some cases internet security limits remote access.

676 **5.1.1.2 Traceability, fiducial reference measurements, changing calibration**

677 Validating satellite observations and numerical models has been a primary objective of NDACC since its inception. Over
678 the past 35 years, the fleet of satellites and their validation needs have evolved significantly. NDACC data meet many
679 of the requirements but not always all.

680 Challenges to the FRM process include outdated standards for uncertainty budgets, e.g., Basher (1982) for Dobsons. For
681 Brewers, calibration relies on several entities: International Ozone Services (IOS), the RBCC-E (Regional Brewer
682 Calibration Center - Europe), and Environment and Climate Change Canada. All three organizations participate in
683 calibration campaigns, publishing results in WMO/GAW reports. There is a high level of agreement, typically 0.5% to
684 1% or better (Zhao et al., 2023), but it is time-consuming to specify data and metadata to ensure reproducible calibrations
685 and efficient reprocessing. The methods developed for more reliable uncertainties (Redondas et al., 2024) are difficult to
686 implement but they represent an opportunity for data format transition, e.g., from NASA Ames to GEOMS-HDF.

687 Spectroscopic reference databases (e.g., HITRAN used in IRWG) are typically updated every 4 years. IWG tracks the
688 effect of changes on NDACC data records to decide on whether to reprocess historical records. An example of ensuring
689 accurate data comes from ozone absorption cross sections used to derive traceable ozone values that have changed several
690 times over ~60 years, i.e., over the lifetime of the Dobson network. NDACC and the larger community have yet to
691 complete the transition to new temperature-dependent cross sections (Serdyuchenko et al., 2014; Weber et al. 2016),
692 approved a decade ago by the International Ozone Commission (Orphal et al., 2016) because implementation requires
693 reprocessing of large archives (Voglmeier et al., 2024). NDACC and WMO/GAW are coordinating the update at the
694 World Ozone and UV Data Center (woudc.org).

695 **5.1.2 Programmatic and infrastructure challenge**

696 **5.1.2.1 Funding challenges**

697 Long-term consistency and continuity are emblematic of NDACC. However, "continue to do for the next five years
698 what was done over the last five years" is not attractive for funders who are oriented toward innovation. NDACC
699 research is heavily driven by instrument PIs and staff who need to diversify their work while also maintaining and



700 expanding their NDACC activities. This is a challenge when funding decreases or when staff move on or retire. With
701 staff changes, institutional priorities may change and a research group is disbanded. NDACC is proactive in
702 overcoming obstacles. NDACC engagement with WMO scientific advisory groups, expert teams and technical
703 conferences, with satellite groups, and with evolving observation strategies, provides support for projects that
704 leverage NDACC measurements as well as for helping individual stations. NDACC's letters to sponsors have
705 prevented station closures. Instrument working group meetings promote visibility of PIs and staff to program
706 managers. NDACC's advances in creating and promulgating standard operating procedures and processing and
707 reprocessing software helps maintain operations as personnel and instruments change.

708 **5.1.2.2 Enhancing network efficiency and expanding NDACC**

709 The focus of NDACC has been on general coordination, and scientific and technical support. Central processing, or very
710 rigid or intrusive requirements, have not been part of NDACC's strategy, although they might make some things more
711 efficient. Over the years, instruments and operating procedures have, however, become more standardized and simpler
712 to operate. NDACCs FTIR stations, for example, use nearly all the same instrument, as well as common traveling
713 calibration standards and operation procedures, which allows processing and species retrieval with a common software
714 and in a central facility for PIs interested in this option. Benefits are more cohesive network-wide data products (e.g.,
715 Hannigan et al., 2022), more timely deposits to data centers, more rapid data reprocessing, retrieval of an increased
716 number of species with greater efficiency, and a reduced burden on station PIs.

717 Another aspect, also from FTIR, is extension of the very high quality but sparse NDACC network to lower quality
718 stations to give better coverage. The standard NDACC high-resolution FTIR interferometers are expensive and require
719 substantial expertise. As a consequence, important portions of the globe are not monitored. Lower cost, moderate spectral
720 resolution (e.g., 2 to 4.5 cm OPD) mid-IR interferometers (Sha et al., 2020), that require little maintenance can provide
721 a solution, especially for tropospheric species or total column abundances (e.g., Zhou et al., 2023). Hardware and
722 software that enable autonomous operation are used. In Kolkata, India, a lower-resolution FTIR instrument provides
723 good quality data for species like HCHO.

724 A world-wide homogeneity among similar instruments within, but also outside NDACC, should be a high priority, e.g.,
725 for global satellite validation and long-term variability analyses. NDACC's ozonesonde community, for example, seeks
726 to increase collaboration with China (e.g., Beijing and Hong Kong) and India (e.g., Pune and Trivandrum), stations that
727 collect a significant number of profiles. However, they use ozonesonde models for which instrumental errors are not
728 fully characterized, e.g. at the World Calibration Centre for Ozone Sondes in Jülich, Germany.

729 More challenging is homogeneity among different instrument types or networks, e.g., for column NO₂, O₃ and HCHO
730 data from NDACC DOAS UV-visible instruments, NDACC FTIRs, and the PGN (Pinardi et al., 2025) or for CH₄, N₂O
731 and CO column data from NDACC FTIR and TCCON (e.g., Zhou et al., 2018; 2019).

732 Easy access to data remains a challenge. The NDACC Data Handling Facility provides access to all NDACC
733 measurements, but formats and versions change over time, and the granularity of data packaging is not always user-
734 friendly. Data archived in multiple centers, in various formats, and with various overlaps among the centers are difficult
735 to use. Examples include ozonesonde data, archived in eight archives (NDACC, WOUDC, SHADOZ, NOAA, EVDC,
736 AVDC, HEGIFTOM, CDS) in different data formats. This leads not only to inconsistencies in data and metadata stored
737 across archives, but between stations in one archive, and even in the data record of one given site. It is expected that



738 transition to unified metadata and data formats, e.g., GEOMS-HDF, will facilitate better coordination among archives.
739 The goal is always to provide simple, friendly access to users, incorporating FAIR principles.

740 **5.2 Scientific opportunities and technical challenges**

741 Challenges and unexpected findings represent new opportunities for NDACC as the following examples illustrate.

742 **5.2.1 Ozone recovery and climate change**

743 Mandates based on the Vienna Convention for the Protection of the Ozone Layer and the associated Montreal Protocol
744 provided the scientific motivation for NDSC in the early 1990s. Following success of the Montreal Protocol and its
745 subsequent amendments (WMO, 2014), there is a common perception that stratospheric ozone depletion is a "solved
746 problem". However, ozone depletion is still substantial and ozone layer recovery is more complex than a decade ago
747 (WMO, 2022), partially due to unexpected increases in very short-lived ODSs into the UT/LS from Asian emissions
748 (e.g., Adcock et al., 2021, Lauther et al., 2022, Pan et al., 2024). These species are only tracked from NDACC ground-
749 based instruments. The need for these data is greater than ever.

750 Related to the need to maintain ODS monitoring for ozone recovery is the impending loss of the MLS water vapor and
751 ClO coverage as well as reduced viewing of Arctic ozone depletion events, volcanic and/or wildfire injections of material
752 into the stratosphere. Springtime stratospheric ozone depletion in polar regions continues to be highly variable year to
753 year (e.g., Manney et al., 2020; Bognar et al., 2021; Pazmino et al., 2023; Shi et al., 2023), making long-term NDACC
754 measurements of ozone-related species important for tracking future changes.

755 **5.2.2 Unexpected events**

756 Unexpected events, such as recent extreme wildfires (Khaykin et al., 2020a; John et al. 2021; Wizenberg et al. 2023;
757 Tickl et al., 2024, Flood et al., 2025, Khaykin et al. 2025) and or the Hunga volcanic eruption (Nedoluha et al., 2023)
758 sharply modified stratospheric composition and perturbed predictions of future stratospheric composition (Strahan et al.,
759 2022; Solomon et al., 2023). Modeling is required to assess impacts of potential injected sulfate particles to the
760 stratosphere, an action designed to counteract global warming. Ongoing climate change has modified the trajectory of
761 ozone recovery (WMO, 2022). Whereas anthropogenic ODS defined NDACC's original measurement portfolio,
762 increasing emissions of GHGs like CO₂, CH₄ and N₂O are re-defining some NDACC priorities. Also relevant are changes
763 in air quality, atmospheric aerosol loading, and cloud cover, for example, affecting surface UV (Cordero et al., 2014;
764 Cordero et al., 2023). Extreme UV events still occur from Antarctic ozone loss, e.g. over Patagonia and the Antarctic
765 peninsula (de Laat et al., 2010; Cordero et al., 2022).

766 **5.2.3 Candidates for expanding NDACC measurements**

767 Generally, as some satellite capabilities decrease and others emerge, NDACC's ground-based measurements remain
768 vital. Examples of expansion opportunities follow.

769 **5.2.3.1 More species from FTIR**

770 NDACC FTIRs at nearly two dozen stations provide clear-sky high-resolution solar absorption measurements for 13 key
771 air quality, ozone, ozone precursors, and greenhouse gases. A strategic aim is to expand this list to more constituents



772 important in climate change, global pollution, and ozone depletion. Potential molecules, already retrieved and archived
773 on the DHF for some FTIR sites, include ammonia (NH_3), ethylene (C_2H_4), methanol (CH_3OH), peroxy-acetyl nitrate
774 (PAN), and hydrofluorocarbons (HFCs) that are regulated by the 2016 Kigali Amendment of the Montreal Protocol.
775 Retrieval of the two most abundant HFCs, HFC-134a and HFC-23, has been demonstrated at a few NDACC stations
776 (Pardo Cantos et al., 2024).

777 **5.2.3.2 Wind**

778 Wind data are vital for weather forecasting and for understanding global circulation, but upper air wind data are scarce.
779 For a short period, the space-based AEOLUS lidar provided global upper atmospheric wind data, greatly improving
780 weather forecasts (Rennie et al. 2021; Garret et al., 2022). Ground-based wind-lidars, a recent NDACC addition (Khaykin
781 et al., 2020b), were instrumental in validating AEOLUS (Ratynski et al., 2023). Microwave radiometers also measure
782 upper atmospheric winds (Hagen et al., 2018). A network of ground-based wind instruments could also validate a space-
783 based wind lidar.

784 **5.2.3.3 Water vapor**

785 Water vapor, the most important greenhouse gas, affects radiation and dynamics, cloud formation and atmospheric
786 chemistry. Climate models show a substantial moist bias in the lowermost stratosphere (Stenke et al, 2007; Charlesworth
787 et al, 2023), a sensitive climate-feedback region. NDACC profiles of water vapor are essential for improving models.
788 NDACC measures high resolution water vapor profiles with balloon-borne FPH and water vapor Raman lidars in the
789 troposphere and (lower) stratosphere (Vömel et al., 2016; Hall et al., 2016; Leblanc et al., 2012; Hicks-Jalali, 2020), as
790 well as coarse resolution profiles in the (upper) stratosphere and mesosphere with microwave radiometers (Nedoluha et
791 al., 2021; 2023). Water vapor measurements for stratospheric needs are usually adequate with monthly or bi-weekly
792 observations.

793 Natural stratospheric water vapor sources, i.e., CH_4 and H_2 oxidation, may be augmented by overshooting convection
794 and subtropical monsoonal circulations. Looking ahead, NDACC has created a water vapor strategy: (https://ndacc.org/under/sites/default/files/2024-01/NDACC_WaterVaporStrategy_20220119.pdf).

796 **5.2.3.4 Aerosols and climate interventions**

797 The stratospheric aerosol layer impacts radiation and chemistry, but stratospheric aerosol is variable, routinely perturbed
798 by small and moderate volcanic eruptions and increasingly by large wildfires (Solomon et al., 2022; Solomon et al, 2023;
799 Peterson et al., 2021). Typical stratospheric aerosol, concentrated between the tropopause and 25 km, is composed of
800 sulfuric acid particles from SO_2 and OCS oxidation, mixed organic sulfate particles that enter from the troposphere, and
801 meteoric particles (Murphy et al., 1998, 2014). Particles from rocket emissions (Katich et al., 2022) and satellite re-entry
802 (Murphy et al., 2023) are likely to increase in the coming decades. The Asian Tropopause Aerosol Layer (Vernier et al.,
803 2011), occurring during boreal summer, contributes up to 15% of Northern Hemisphere aerosol (Yu et al., 2017). Recent
804 NDACC aerosol measurements show that the Asian summer monsoon is a weak but a measurable source of Arctic
805 stratospheric aerosol even in the Arctic from late summer to early autumn (Graßl et al., 2024). Routine measurements of
806 stratospheric aerosol, a key capability of NDACC, are essential, particularly if climate intervention leads to enhanced
807 particle injections (Asher et al., 2023) and large wildfires (Asher et al., 2024). Because size distributions are not directly
808 observable from space, measurements of particle composition are frequently carried out during aircraft campaigns.



809 NDACC proposes to add routine balloon-borne measurements of aerosol size distributions with optical particle
810 spectrometers, e.g., the Portable Optical Particle Spectrometer (POPS; Todt et al., 2023) in the next 3-5 years.

811 **6 Outlook**

812 This article has reviewed the fundamentals of NDACC, its rationale, mission and the success of the highest quality
813 instruments in monitoring atmospheric composition and contributing to major assessments. NDACC's Working Groups
814 have been exemplary in promulgating standards and best practices. Similar approaches have been employed by
815 NDACC's 10 Cooperating Networks. NDACC has been active in research and scientific service programs, especially
816 within the European Union and North America, and within international satellite projects where its data are essential to
817 algorithm and model development and validation. NDACC is operating within the framework of the latest developments
818 in data distribution and management practices.

819 NDACC's impact on solving major problems in atmospheric composition and climate has been highlighted. For example,
820 long-term monitoring has been foundational in tracking the health of the stratospheric ozone layer and more recently, the
821 evolution of air quality and climate pollutants. Exceptional events, such as volcanic eruptions, are captured with NDACC
822 observations, which can measure impacts on a scale too small for satellites. With a decreasing satellite constellation for
823 stratospheric composition, the need for NDACC observations could not be greater. NDACC is at a crossroads as resource
824 pressures on ground-based monitoring programs increase. With data archiving and distribution activities diverting
825 resources from data collection in some networks, strategic planning is essential to strengthen NDACC and its
826 Cooperating Networks.

827 Based on specific recommendations in prior sections, NDACC is well-positioned to adopt a three-pronged strategy:
828 protect existing stations and data streams; promote greater usage of NDACC data; and expand NDACC's coverage
829 geographically and in species-parameter space.

830 **Protect Existing Stations and Data streams.** As described above, current NDACC observing infrastructure and
831 resources (instruments, data, and people) must be sustained. With many stations operating for three to four decades, their
832 records are increasingly indispensable as the value of a dataset increases with its longevity. NDACC and cooperating
833 partners are actively engaging a younger generation of scientists and technical professionals, with a specific focus on
834 expanding representations from underrepresented areas. The goal is to evolve infrastructure so that expertise and projects
835 are transferred, that capacity is built, and that innovative ideas and insights emerge. An important element of this effort
836 is the ongoing development of more cost-effective and automated instruments, with centralized data acquisition and
837 processing. Adding new observations at existing stations, leveraging infrastructure and personnel, is another approach to
838 strengthening the networks.

839 **Promote Greater Usage of NDACC Data:** It is important to advertise and promote the usage of the NDACC data with
840 network stakeholders and throughout the global scientific community. Due to its roots in stratospheric ozone research,
841 including development and validation of satellite products, there is a dedicated data user group worldwide that extends
842 to atmospheric dynamics and air quality. NDACC is currently extending data impact through cross-disciplinary
843 initiatives in climate and carbon cycle research, climate intervention, etc. The efforts of NDACC and cooperating
844 networks to distribute data more rapidly and more accessibly, conforming to the latest data practices (e.g., FAIR), are



845 widening impact even more, as are data sharing initiatives with WMO and other organizations. The CAMS assimilation
846 system that relies on NDACC observations as an independent reference is another sign of network impact. The TOAR
847 II HEGIFTOM activity, with data reprocessing from four NDACC instrument types, marks a major milestone. The
848 HEGIFTOM archive, which will be entirely harboured on the NDACC DHF and other historical archives, is now a gold
849 standard, supplying reference data for evaluation of satellite products and global model output. More active collaboration
850 with satellite and modeling communities will further promote applications of NDACC data.

851 **Expand NDACC's coverage in two ways:**

852 Geographical Coverage. NDACC's coverage is still poor in Africa, Asia, South America and the Mediterranean region,
853 partly due to shortage of resources for equipment and of skilled personnel or expertise. In other cases, high-quality data
854 are collected but they are not shared. The latter situation is expected to improve over time as more journals publish links
855 to data archives. NDACC needs to engage with organizations that have infrastructure and expertise. An NDACC
856 affiliation is a path to greater visibility and access to unique expertise and support.

857 Collaborations within Cooperating Networks, WMO/GAW, and other agencies can be leveraged to augment NDACC
858 stations. Finding a means of incorporating data from environmental and air quality agencies is an approach to consider.
859 Note the success of the TOAR tropospheric ozone archive. A compelling rationale for expanding NDACC to more urban
860 stations is that researchers evaluating satellite products for air quality and emissions estimates are a growing user
861 community for our data.

862 Coverage of Species and Parameters (Variables Space). NDACC needs to add measurements of species that are coming
863 to greater prominence, or that may not have existed or been measurable decades ago. Selection criteria must include the
864 added-value and complementarity with existing observations at a given station. NDACC instrument working groups,
865 laboratory spectroscopists, and instrument developers can support this work. With the advent of constellations of nadir-
866 looking satellites focusing on air quality pollutants and greenhouse gas observations, including those from geostationary
867 platforms, and the NRT assimilation of their data in forecast systems, we must ensure that observations are carried out
868 and assimilated as continuously as possible. The increasing automation and rapid distribution capacity of NDACC
869 observations is a must for these operations. NDACC is ready to face its future evolution and is confident that the network
870 will maintain and even strengthen its relevance provided that the required resources can be leveraged.

871 NDACC has faced, and will continue to face, challenges. However, the combined experience and substantial know-how
872 of NDACC's PIs, instrument working groups, and its associated networks should overcome these challenges, develop
873 new opportunities, and secure the continuation of the 35+ years of high-quality, long-term measurements that NDACC
874 is known for. Ground-based data remain irreplaceable for documenting key aspects of atmospheric composition in a
875 warming troposphere and a cooling stratosphere.

876 **Appendix A. NDACC Organizational structure.**

877 **Figure A1. Organizational structure of NDACC.**

878



879

880 **Appendix B. Spectral Range of NDACC observations.**

881 **Table B1. Definition of Solar spectral range used in the NDACC observations. See full instrument description at**
 882 <https://ndacc.larc.nasa.gov/instruments>.

Name & Spectral Range	Working Group & Cooperating Network	Instrumentation
UV (Ultra-Violet) 200 - 400 nm	Brewer, Dobson, UV Spectroradiometer, UV/Vis Spectrometer	Dobson, Brewer, SAOZ, MAX-DOAS, SUV-100, SUV-150B, JYHD10, Bentham (DTM300, DTMC300, DTM300V, DM150), UV (5, 6, 7), Lidar (DIAL, Rayleigh, Raman)
VIS (Visible) 400 - 700 nm	AERONET, BSRN, EuBrewNet, MPLNet, PGN, TOLNet	
NIR (Near IR) ~700 nm - 2 μm	COCCON, TCCON, AERONET	Bruker 120HR, Bruker EM-27
MIR (Middle Infra-Red) ~2.0 - 14.3 μm	IRWG	Bruker (120, 120M, 125M, 120HR, 125HR), JPL MkIV, Bomem (DA2, DA3, DA8), EOCOM, McMath FTS
MW (Microwave) 13.47 mm - 1.08 mm	MWWG	MIAWARA, MIAWARA-C, GROMOS, GROMOS-C, SOMORA, WIRA, WIRA-C



883 **Appendix C. List of satellite validation work and collaborative effort.**

884 **Table C1. recent and current satellite missions for which NDACC provides validation data and / or collaboration effort. Sect.**
885 **3.4 gives more details on present and upcoming missions.**

Satellite / Sensor	Product	NDACC Group	Reference paper
SAGE III / ISS	H ₂ O	Lidar, O ₃ sonde	Davis et al., 2021 Wang et al., 2020
	O ₃	Lidar, O ₃ sonde	Johnson et al., 2024, Mettig et al., 2022, Mettig et al., 2021
Terra/MOPITT	CO	IRWG	Gaubert et. al., 2023 ; Lutsch et. al., 2022 ; Buchholz et. al., 2017 ; Jalali et al., 2022
TEMPO	HCHO	IRWG, UV-VIS	Souri et al., 2023
	NO ₂	IRWG, UV-VIS	Souri et al., 2023
	O ₃	Lidar	Johnson et al., 2018
TEMPO+GEMS	O ₃ (tot)	Brewer/Dobson	Zhao et al., 2025
GEMS	HCHO	IRWG, UV-VIS	Lee et al., 2023
NPP/CrIS	CH ₃ OH, C ₂ H ₂ , C ₂ H ₄ , C ₅ H ₈ , HCN	IRWG	Wells et al., 2022, Wells et al., 2024, Brewer et al., 2024 Wells et al. 2025
IASI	N ₂ O	IRWG	Barrret et al., , 2021 Vandenbussche et. al., 2022
	CO	IRWG	Langerock et al., 2023
	HNO ₃	IRWG	Langerock et al., 2023
	CH ₄	IRWG	Dils et al., 2024
	PAN	IRWG	Mahieu et al., 2021; Wizenberg et al., 2022; Wizenberg et al., 2023
	HCOOH	IRWG	Franco et al., 2020; Franco et al., 2021
	H ₂ CO	IRWG	Kwon et al., 2023
Aura/MLS	T	Lidar; MWG	Chen et al., 2023; Navas-Guzman et al, 2017
	O ₃	MWG	Maillard Barras et al, 2020; Sauvageat et al, 2022
	CIO	MWG	Nedoluha et al., 2025
	H ₂ O	MWG	Nedoluha et al., 2022; Bell et al, 2025
		SWG, MWG	Livesey et al., 2021



SCISAT/ACE	N2O	IRWG	Minganti et al, 2021
	inorganic fluorine	IRWG	Prignon et al., 2021
AURA /OMI	O3	SWG	Huang et al., 2017, Bak et al., 2024
	HCHO	RWGI, UV-VIS	De Smedt et al. (2021); Ayazpour et al., 2025; Müller et al., 2024
SAGE III/ISS	Ozone, WV	Lidar, O3sonde	Wang et al., 2020
	Aerosol	Lidar	Knepp et al., 2020
	H2O	SWG	Davis et al., 2021
GOME-2	OCIO	UV-VIS	Pinardi et al., 2022
FengYun-3E/HIRAS-II	CO, HCOOH, PAN	IRWG	Hua et al., 2025
Copernicus S5P	H2CO	IRWG, UV-VIS	De Smedt et al. (2021), Oomen et al., 2024, Müller et al., 2024
	CH4	IRWG	Sha et al (2021)
	O3	IRWG, SWG	Vigouroux et al. 2020, Keppens et al., 2024
	NO2	UV-VIS	Verhoelst et al., 2021

887

888



889 **Data Availability**

890 The NDACC data used in this paper are archived at the Data Host Facility (DHF) that is hosted at NASA Langley
891 Research Center (LaRC). DHF is serving as a central archive and access point for atmospheric data, offering tools for
892 scientists to query and download datasets related to ozone, aerosols, and other atmospheric components: [https://www-](https://www-air.larc.nasa.gov/missions/ndacc/)
893 [air.larc.nasa.gov/missions/ndacc/](https://www-air.larc.nasa.gov/missions/ndacc/)

894 **Author contributions**

895 MD, JCL, IP and JW conceptualized the paper. IP, MD, JW, AT, HS, JWH, RH, WS and JCL led the paper preparation.
896 All authors contributed to the writing of the paper and/or provided figures either from their published papers or updated
897 published figures.

898 **Competing interests**

899 At least one of the (co-)authors is a member of the editorial board of Atmospheric Chemistry and Physics.

900 **Disclaimer**

901 The statements, findings, conclusions, and recommendations are those of the author(s) and do not necessarily reflect the
902 views of NOAA or the U.S. Department of Commerce.

903 **Acknowledgements**

904 This work has been supported in part by NOAA (grant no. NA19NES4320002; Cooperative Institute for Satellite Earth
905 System Studies – CISESS) at the University of Maryland/ESSIC and NOAA (grant no. NA22OAR4320151) for the
906 Cooperative Institute for Earth System Research and Data Science (CIESRDS). Emmanuel Mahieu is a research director
907 with F.R.S.-FNRS (Brussels, Belgium). Cloud and radiation measurements within NDACC are supported by DFG, which
908 funds the project "Cloud 3D Structure and Radiation (C3SAR). JWH & IO at the National Center for Atmospheric
909 Research are sponsored by the National Science Foundation. The NCAR NDACC program are supported under contract
910 by the National Aeronautics and Space Administration (NASA).

911 **Financial support**

912 This research has been supported in part by NOAA (grant no. NA19NES4320002; Cooperative Institute for Satellite
913 Earth System Studies – CISESS) at the University of Maryland/ESSIC and NOAA (grant no. NA22OAR4320151) for
914 the Cooperative Institute for Earth System Research and Data Science (CIESRDS). GMI and the GEOS CCM were
915 supported by the NASA Modeling, Analysis, and Prediction program and the GEOS-GMI MINDS simulation was



916 supported by the NASA MEaSURES program and computational resources from the NASA Center for Climate
917 Simulation.

918 **References**

919 Adcock, K. E., Fraser, P. J., Hall, B. D., Langenfelds, R. L., Lee, G., Montzka, S. A., Oram, D. E., Rockmann, T., Stroh,
920 F., Sturges, W. T., Vogel, B., and Laube, J. C. (2021). Aircraft-Based Observations of Ozone-Depleting Substances in
921 the Upper Troposphere and Lower Stratosphere in and Above the Asian Summer Monsoon. *J. Geophys. Res.*, **126**,
922 e2020JD033137. <https://doi.org/10.1029/2020JD033137>.

923 Asher E, Baron A, Yu P, Todt M, Smale P, Liley B, Querel R, Sakai T, Morino I, Jin Y, Nagai T, Uchino O, Hall E,
924 Cullis P, Johnson B, and Thornberry TD: Balloon baseline stratospheric aerosol profiles (B2SAP)—perturbations in the
925 southern hemisphere, 2019–2022, *J. Geophys. Res.-Atmos.*, **129**, e2024JD041581, 2024.
926 <https://doi.org/10.1029/2024JD041581>

927 Asher E, Todt M, Rosenlof K, Thornberry T, Gao R, Taha G, Walter P, Alvarez S, Flynn J, Davis S, Evan S, Brioude J,
928 Metzger J-M, Hurst DF, Hall E, and Xiong K (2023), Unexpectedly rapid aerosol formation in the Hunga Tonga plume,
929 *Proc. Natl. Acad. Sci.*, **120**, e2219547120, <https://doi.org/10.1073/pnas.2219547120>

930 Agustí-Panareda, A., Barré, J., Massart, S., Inness, A., Aben, I., Ades, M., Baier, B. C., Balsamo, G., Borsdorff, T.,
931 Bousserez, N., Boussetta, S., Buchwitz, M., Cantarello, L., Crevoisier, C., Engelen, R., Eskes, H., Flemming, J.,
932 Garrigues, S., Hasekamp, O., Huijnen, V., Jones, L., Kipling, Z., Langerock, B., McNorton, J., Meilhac, N., Noël, S.,
933 Parrington, M., Peuch, V.-H., Ramonet, M., Razinger, M., Reuter, M., Ribas, R., Suttie, M., Sweeney, C., Tarniewicz,
934 J., and Wu, L.: Technical note: The CAMS greenhouse gas reanalysis from 2003 to 2020, *Atmos. Chem. Phys.*, **23**,
935 3829–3859, <https://doi.org/10.5194/acp-23-3829-2023>, 2023.

936 Ayazpour, Z., González Abad, G., Nowlan, C. R., Sun, K., Kwon, H.-A., Chan Miller, C., et al. (2025). Aura ozone
937 monitoring instrument (OMI) Collection 4 formaldehyde products. *Earth and Space Science*, **12**, e2024EA003792.
938 <https://doi.org/10.1029/2024EA003792>

939 Bak, J., Liu, X., Yang, K., Gonzalez Abad, G., O'Sullivan, E., Chance, K., and Kim, C.-H.: An improved OMI ozone
940 profile research product version 2.0 with collection 4 L1b data and algorithm updates, *Atmos. Meas. Tech.*, **17**, 1891–
941 1911, <https://doi.org/10.5194/amt-17-1891-2024>, 2024.

942 Ball, WT, Krivošova N, Rozanov E V., et al. (2018). The Upper Troposphere and Lower Stratosphere as a key region
943 for future tropical ozone, *Atmos. Chem. Phys.*, **18**, 1379–1392, <https://doi.org/10.5194/acp-18-1379-2018>

944 Baron, A., Chazette, P., Khaykin, S., Payen, G., Marquestaut, N., Bégué, N., and Duflot, V. (2023). Early evolution of
945 the stratospheric aerosol plume following the 2022 Hunga Tonga-Hunga Ha'apai eruption: Lidar observations from
946 Reunion (21°S, 55°E). *Geophysical Research Letters*, **50**, e2022GL101751.

947 Barret B, Gouzenes Y, Le Flochmoen E, Ferrant S. Retrieval of Metop-A/IASI N2O Profiles and Validation with
948 NDACC FTIR Data. *Atmosphere*. 2021; **12**(2):219. <https://doi.org/10.3390/atmos12020219>

949 Basher, R. E. (1982): “Review of the Dobson spectrophotometer and its accuracy”, WMO Global Ozone Research and
950 Monitoring, Report No. 13, Geneva, Switzerland. <https://gml.noaa.gov/ozwv/dobson/papers/report13/report13.html> (last
951 access: 11 April 2024).



952 Bell, A., Sauvageat, E., Stober, G., Hocke, K., and Murk, A.: Developments on a 22 GHz microwave radiometer and
953 reprocessing of 13-year time series for water vapour studies, *Atmos. Meas. Tech.*, **18**, 555–567,
954 <https://doi.org/10.5194/amt-18-555-2025>, 2025.

955 Bernhard, G., & Stierle, S. (2020). Trends of UV radiation in Antarctica. *Atmosphere*, **11**(8), 795.

956 Bernhard, G.H., Bais, A.F., Aucamp, P.J. et al. Stratospheric ozone, UV radiation, and climate interactions. *Photochem
957 Photobiol Sci* **22**, 937–989 (2023). <https://doi.org/10.1007/s43630-023-00371-y>

958 Bjorklund, R., Vigouroux, C., Effertz, P., García, O. E., Geddes, A., Hannigan, J., Miyagawa, K., Kotkamp, M.,
959 Langerock, B., Nedoluha, G., Ortega, I., Petropavlovskikh, I., Poyraz, D., Querel, R., Robinson, J., Shiona, H., Smale,
960 D., Smale, P., Van Malderen, R., and De Maziere, M. (2024). Intercomparison of long-term ground-based measurements
961 of total, tropospheric, and stratospheric ozone at Lauder, New Zealand. *Atmos. Meas. Tech.*, **17**, 6819–6849.
962 <https://doi.org/10.5194/amt-17-6819-2024>.

963 Bognar, K., Alwarda, R., Strong, K., Chipperfield, M. P., Dhomse, S. S., Drummond, J. R., et al. (2021). Unprecedented
964 spring 2020 ozone depletion in the context of 20 years of measurements at Eureka, Canada. *Journal of Geophysical
965 Research: Atmospheres*, **126**, e2020JD034365. <https://doi.org/10.1029/2020JD034365>

966 Boone, C. D., Bernath, P. F., and Fromm, M. D. (2020). Pyrocumulonimbus stratospheric plume injections measured by
967 the ACE-FTS. *Geophysical Research Letters*, **47**(15), e2020GL088442.

968 Brewer, J.F., Millet, D.B., Wells, K.C. et al. Space-based observations of tropospheric ethane map emissions from fossil
969 fuel extraction. *Nat Commun* **15**, 7829 (2024). <https://doi.org/10.1038/s41467-024-52247-z>

970 Broderick, A. J., and T. M. Hard. (1974). Proceedings of the Third Conference on the Climatic Impact Assessment
971 Program, February 26-March 1, 1974. U. S. Dept. of Transportation, Cambridge, MA, 672 pp.
972 <https://ntrs.nasa.gov/NTRL/dashboard/searchResults/titleDetail/ADA003846.xhtml#>.

973 Brewer, J.F., Millet, D.B., Wells, K.C. et al. Space-based observations of tropospheric ethane map emissions from fossil
974 fuel extraction. *Nat Commun* **15**, 7829 (2024). <https://doi.org/10.1038/s41467-024-52247-z>

975 Brogniez, C., Doré, J. F., Auriol, F., Cesarini, P., Minvielle, F., Deroo, C., & Da Conceicao, P. (2021). Erythemal and
976 vitamin D weighted solar UV dose-rates and doses estimated from measurements in mainland France and on Reunion
977 Island. *Journal of Photochemistry and Photobiology B: Biology*, **225**, 112330.

978 Buchholz, J., Querner, P., Paredes, D. et al. Soil biota in vineyards are more influenced by plants and soil quality than
979 by tillage intensity or the surrounding landscape. *Sci Rep* **7**, 17445 (2017). <https://doi.org/10.1038/s41598-017-17601-w>

980 Charlesworth, E., Ploger, F., Birner, T., Baikhadzhaev, R., Abalos, M., Abraham, N. L., Akiyoshi, H., Bekki, S.,
981 Dennison, F., Jockel, P., Keeble, J., Kinnison, D., Morgenstern, O., Plummer, D., Rozanov, E., Strode, S., Zeng, G.,
982 Egorova, T. & Riese, M. (2023). Stratospheric water vapor affecting atmospheric circulation. *Nat Commun* **14**, 3925.

983 Chen, Z., Schwartz, M. J., Bhartia, P. K., Schoeberl, M., Kramarova, N., Jaross, G., and DeLand, M. (2023). Mesospheric
984 and upper stratospheric temperatures from OMPS-LP. *Earth and Space Science*, **10**(5):e2022EA002763.

985 Chipperfield, M. P., Hegglin, M. I., A., M. S., Newman, P. A., Park, S., Reimann, S., Rigby, M., Stohl, A., Velders, G.
986 J. M., Walter-Terrinoni, H. and Yao, B. (2021). **Report on the Unexpected Emissions of CFC-11**.

987 Chipperfield, M. P., Liang, Q., Rigby, M., Hossaini, R., Montzka, S. A., Dhomse, S., Feng, W., Prinn, R. G., Weiss, R.
988 F., Harth, C. M., Salameh, P. K., Muhle, J., O'Doherty, S., Young, D., Simmonds, P. G., Krummel, P. B., Fraser, P. J.,
989 Steele, L. P., Happell, J. D., Rhew, R. C., Butler, J., Yvon-Lewis, S. A., Hall, B., Nance, D., Moore, F., Miller, B. R.,



990 Elkins, J. W., Harrison, J. J., Boone, C. D., Atlas, E. L. and Mahieu, E. (2016). Model sensitivity studies of the decrease
991 in atmospheric carbon tetrachloride. *Atmos. Chem. Phys.*, **16**(24), 15741–15754. doi:10.5194/acp-16-15741-2016.

992 Chouza, F., Leblanc, T., Brewer, M., Wang, P., Martucci, G., Haefele, A., Vérèmes, H., Duflot, V., Payen, G., and
993 Keckhut, P.: The impact of aerosol fluorescence on long-term water vapor monitoring by Raman lidar and evaluation of
994 a potential correction method, *Atmos. Meas. Tech.*, **15**, 4241–4256, <https://doi.org/10.5194/amt-15-4241-2022>, 2022.

995 Chouza, F., Leblanc, T., Wang, P., Brown, S. S., Zuraski, K., Chace, W., Womack, C. C., Peischl, J., Hair, J., Shingler,
996 T., and Sullivan, J.: The Small Mobile Ozone Lidar (SMOL): instrument description and first results, *Atmos. Meas.*
997 *Tech.*, **18**, 405–419, <https://doi.org/10.5194/amt-18-405-2025>, 2025.

998 Compernolle, S., A. Argyrouli, R. Lutz, M. Sneep, J.-C. Lambert, A. M. Fjaeraa, D. Hubert, A. Keppens, D. Loyola, E.
999 O'Connor, F. Romahn, P. Stammes, T. Verhoelst, and P. Wang, Validation of the Sentinel-5 Precursor TROPOMI cloud
1000 data with Cloudnet, Suomi-NPP VIIRS and OMI O2-O2 (2021). *Atmos. Meas. Tech.*, Vol. **14**, 2451–2476,
1001 <https://doi.org/10.5194/amt-14-2451-2021>

1002 Cordero R. R., Feron S., Damiani A., Sepúlveda E., Jorquera J., Redondas A., Seckmeyer G., Carrasco J., Rowe P.,
1003 Ouyang Z. (2023). Surface Solar Extremes in the Most Irradiated Region on Earth, Altiplano. *Bulletin of the American*
1004 *Meteorological Society (BAMS)*. DOI 10.1175/BAMS-D-22-0215.1.

1005 Cordero, R. R., Feron, S., Damiani, A., Redondas, A., Carrasco, J., Sepúlveda, E., & Seckmeyer, G. (2022). Persistent
1006 extreme ultraviolet irradiance in Antarctica despite the ozone recovery onset. *Scientific reports*, **12**(1), 1266.
1007 <https://doi.org/10.1038/s41598-022-05449-8>.

1008 Cordero, R.R., Seckmeyer, G., Damiani, A. et al. (2014). The world's highest levels of surface UV. *Photochem Photobiol*
1009 *Sci* **13**, 70-81. <https://doi.org/10.1039/c3pp50221j>.

1010 Dammers, E., Vigouroux, C., Palm, M., Mahieu, E., Warneke, T., Smale, D., Langerock, B., Franco, B., Van Damme,
1011 M., Schaap, M., Notholt, J., and Erisman, J. W.: Retrieval of ammonia from ground-based FTIR solar spectra, *Atmos.*
1012 *Chem. Phys.*, **15**, 12789–12803, <https://doi.org/10.5194/acp-15-12789-2015>, 2015.

1013 Davis, S. M., Damadeo, R., Flittner, D., Rosenlof, K. H., Park, M., Randel, W. J., et al. (2021). Validation of SAGE
1014 III/ISS solar water vapor data with correlative satellite and balloon-borne measurements. *Journal of Geophysical*
1015 *Research: Atmospheres*, **126**, e2020JD033803. <https://doi.org/10.1029/2020JD033803>

1016 De Mazière, et al. (2018). The Network for the Detection of Atmospheric Composition Change (NDACC): history, status
1017 and perspectives. *Atmos. Chem. Phys.*, **18**, 4935. <https://doi.org/10.5194/acp-18-4935-2018>.

1018 de Laat, A. T. J., R. J. van der A, M. A. F. Allaart, M. van Weele, G. C. Benitez, C. Casiccia, N. M. Paes Leme, E. Quel,
1019 J. Salvador, and E. Wolfram (2010), Extreme sunbathing: Three weeks of small total O3 columns and high UV radiation
1020 over the southern tip of South America during the 2009 Antarctic O3 hole season. *Geophys. Res. Lett.*, **37**, L14805.
1021 doi:10.1029/2010GL043699.

1022 De Smedt, I., Pinardi, G., Vigouroux, C., Compernolle, S., Bais, A., Benavent, N., Boersma, F., Chan, K.-L., Donner,
1023 S., Eichmann, K.-U., Hedelt, P., Hendrick, F., Irie, H., Kumar, V., Lambert, J.-C., Langerock, B., Lerot, C., Liu, C.,
1024 Loyola, D., Piters, A., Richter, A., Rivera Cárdenas, C., Romahn, F., Ryan, R. G., Sinha, V., Theys, N., Vlietinck, J.,
1025 Wagner, T., Wang, T., Yu, H., and Van Roozendael, M.: Comparative assessment of TROPOMI and OMI formaldehyde
1026 observations and validation against MAX-DOAS network column measurements, *Atmos. Chem. Phys.*, **21**, 12561–
1027 12593, <https://doi.org/10.5194/acp-21-12561-2021>, 2021.



1028 Dils, B., Zhou, M., Camy-Peyret, C., De Mazière, M., Kangah, Y., Langerock, B., Prunet, P., Serio, C., Siddans, R., and
1029 Kerridge, B.: Independent validation of IASI/MetOp-A LMD and RAL CH₄ products using CAMS model, in situ
1030 profiles, and ground-based FTIR measurements, *Atmos. Meas. Tech.*, 17, 5491–5524, <https://doi.org/10.5194/amt-17-5491-2024>, 2024.

1032 Duncan, B. N., Strahan, S. E., Yoshida, Y., Steenrod, S. D., and Livesey, N. (2007). Model study of the cross-tropopause
1033 transport of biomass burning pollution. *Atmos. Chem. Phys.*, 7, 3713–3736. <https://doi.org/10.5194/acp-7-3713-2007>.

1034 Evan, S., et al. (2023). Rapid ozone depletion after humidification of the stratosphere by the Hunga Tonga eruption.
1035 *Science*, 382, 282. <https://doi.org/10.1126/science.adg2551>.

1036 Evan et al 2023. <https://doi.org/10.1126/science.adg2551>. (Duplicate of previous Evan entry, kept for reference).

1037 Fisher, B.L., Lamsal, L.N., Fasnacht, Z., Oman, L.D., Joiner, J., Krotkov, N.A., Choi, S., Qin, W. and Yang, E.S. (2024).
1038 Revised estimates of NO₂ reductions during the COVID-19 lockdowns using updated TROPOMI NO₂ retrievals and
1039 model simulations. *Atmospheric Environment*, 326, 120459.

1040 Flood et al., 2025. <https://doi.org/10.1029/2024JD042254>.

1041 Franco, B., Clarisse, L., Stavrakou, T., Müller, J.-F., Taraborrelli, D., Hadji-Lazaro, J., et al. (2020). Spaceborne
1042 measurements of formic and acetic acids: A global view of the regional sources. *Geophysical Research Letters*, 47,
1043 e2019GL086239. <https://doi.org/10.1029/2019GL086239>.

1044 Franco B., Blumenstock T., Cho C., Clarisse L., Clerbaux C., Coheur P.F., De Mazière M., De Smedt I., Dorn H.P.,
1045 Emmerichs T., Fuchs H., Gkatzelis G., Griffith D.W.T., Hannigan J.W., Hase F., Jones N., Kerkweg A., Kiendler-Scharr
1046 A., Mahieu E., Novelli A., Ortega I., Paton-Walsh C., Pommier M., Pozzer A., Reimer D., Rosanka S., Sander R.,
1047 Schneider M., Strong K., Tillmann R., Van Roozendael M., Vereecken L., Vigouroux C., Wahner A., Taraborrelli D.
1048 (2021). Ubiquitous atmospheric production of organic acids mediated by cloud droplets. *Nature*, 593(7858), 233–237.
1049 doi:10.1038/s41586-021-03462-x.

1050 Garane, K., Koukouli, M.-E., Verhoelst, T., Fioletov, V., Lerot, C., Heue, K.-P., Bais, A., Balis, D., Bazureau, A., Dehn,
1051 A., Goutail, F., Granville, J., Griffin, D., Hubert, D., Keppens, A., Lambert, J.-C., Loyola, D., McLinden, C., Pazmino,
1052 A., Pommereau, J.-P., Redondas, A., Romahn, F., Valks, P., Van Roozendael, M., Xu, J., Zehner, C., Zerefos, C., and
1053 Zimmer, W. (2019). TROPOMI/S5P total ozone column data: global ground-based validation & consistency with other
1054 satellite missions, *Atmos. Meas. Tech.*, <https://doi.org/10.5194/amt-2019-147>

1055 Garrett, K., Liu, H., Ide, K., Hoffman, R.N. & Lukens, K.E. (2022). Optimization and impact assessment of Aeolus
1056 HLOS wind assimilation in NOAA's global forecast system. *Quarterly Journal of the Royal Meteorological Society*,
1057 148(747), 2703–2716. <https://doi.org/10.1002/qj.4331>.

1058 Gaubert, B., Stephens, B. B., Baker, D. F., Basu, S., Bertolacci, M., Bowman, K. W., et al. (2023). Neutral tropical
1059 African CO₂ exchange estimated from aircraft and satellite observations. *Global Biogeochemical Cycles*, 37,
1060 e2023GB007804. <https://doi.org/10.1029/2023GB007804>

1061 Gaudel, A., O. R. Cooper, et al. (2018). Tropospheric Ozone Assessment Report: Present-day distribution and trends of
1062 tropospheric ozone relevant to climate and global atmospheric chemistry model evaluation. *Elem. Sci. Anth.*, 6(1):39.
1063 doi: <https://doi.org/10.1525/elementa.291>.

1064 Gaudel, A., Bourgeois, I., Li, M., Chang KL et al: Tropical tropospheric ozone distribution and trends from in situ and
1065 satellite data, *Atmos. Chem. Phys.*, <https://doi.org/10.5194/acp-24-9975-2024>



1066 Gelaro, R., McCarty, W., Suárez, M.J., Todling, R., Molod, A., Takacs, L., Randles, C.A., Darmenov, A., Bosilovich,
1067 M.G., Reichle, R. and Wargan, K. (2017). The modern-era retrospective analysis for research and applications, version
1068 2 (MERRA-2). *Journal of Climate*, **30**(14), 5419–5454.

1069 Godin-Beekmann, S., Azouz, N., Sofieva, V. F., Hubert, D., Petropavlovskikh, I., Effertz, P., Ancellet, G., Degenstein,
1070 D. A., Zawada, D., Froidevaux, L., Frith, S., Wild, J., Davis, S., Steinbrecht, W., Leblanc, T., Querel, R., Tourpali, K.,
1071 Damadeo, R., Maillard Barras, E., Stübi, R., Vigouroux, C., Arosio, C., Nedoluha, G., Boyd, I., Van Malderen, R.,
1072 Mahieu, E., Smale, D., and Sussmann, R.: Updated trends of the stratospheric ozone vertical distribution in the 60° S–
1073 60° N latitude range based on the LOTUS regression model , *Atmos. Chem. Phys.*, **22**, 11657–11673,
1074 https://doi.org/10.5194/acp-22-11657-2022, 2022.

1075 Goldman, A., Paton-Walsh, C., Bell, W., Toon, G., Blavier, J., Sen, B., Coffey, M., Hannigan, J., and Mankin, W. (1999).
1076 Network for the Detection of Stratospheric Change Fourier Transform Infrared Intercomparison at Table Mountain
1077 Facility, November 1996. *Journal of Geophysical Research-Atmospheres*, **104**(D23):30481–30503.

1078 Goryl, P.; Fox, N.; Donlon, C.; Castracane, P. (2023). Fiducial Reference Measurements (FRMs): What Are They?
1079 *Remote Sensing*, **15**(20), 5017. <https://doi.org/10.3390/rs15205017>.

1080 Graßl, S., Ritter, C., Tritscher, I., and Vogel, B.: Does the Asian summer monsoon play a role in the stratospheric aerosol
1081 budget of the Arctic?, *Atmos. Chem. Phys.*, **24**, 7535–7557, https://doi.org/10.5194/acp-24-7535-2024, URL
1082 https://acp.copernicus.org/articles/24/7535/2024/, 2024.

1083 Grooß, J.-U., Müller, R., Crowley, J. N., & Hegglin, M. I. (2025). Chlorine peroxide reaction explains observed
1084 wintertime hydrogen chloride in the antarctic vortex. *Communications Earth & Environment*, **6**(1), 1–8.

1085 Hagen, J., Murk, A., Rüfenacht, R., Khaykin, S., Hauchecorne, A., and Kämpfer, N. (2018). WIRA-C: a compact 142-
1086 GHz-radiometer for continuous middle-atmospheric wind measurements. *Atmos. Meas. Tech.*, **11**, 5007–5024.
1087 <https://doi.org/10.5194/amt-11-5007-2018>.

1088 Hall, E. G., Jordan, A. F., Hurst, D. F., Oltmans, S. J., Vömel, H., Kühnreich, B., and Ebert, V.: Advancements,
1089 measurement uncertainties, and recent comparisons of the NOAA frost point hygrometer, *Atmos. Meas. Tech.*, **9**, 4295–
1090 4310, https://doi.org/10.5194/amt-9-4295-2016, 2016.

1091 Hannigan, J. W., Ortega, I., Shams, S. B., Blumenstock, T., Campbell, J. E., Conway, S., et al. (2022). Global atmospheric
1092 OCS trend analysis from 22 NDACC stations. *Journal of Geophysical Research: Atmospheres*, **127**, e2021JD035764.
1093 <https://doi.org/10.1029/2021JD035764>.

1094 Herman, J., Evans, R., Cede, A., Abuhassan, N., Petropavlovskikh, I., and McConville, G. (2015). Comparison of ozone
1095 retrievals from the Pandora spectrometer system and Dobson spectrophotometer in Boulder, Colorado. *Atmos. Meas.
1096 Tech.*, **8**, 3407–3418. <https://doi.org/10.5194/amt-8-3407-2015>.

1097 Herrera, B., Bezanilla, A., Blumenstock, T., Dammers, E., Hase, F., Clarisse, L., Magaldi, A., Rivera, C., Stremme, W.,
1098 Strong, K., Viatte, C., Van Damme, M., and Grutter, M.: Measurement report: Evolution and distribution of NH₃ over
1099 Mexico City from ground-based and satellite infrared spectroscopic measurements, *Atmos. Chem. Phys.*, **22**, 14119–
1100 14132, https://doi.org/10.5194/acp-22-14119-2022, 2022.

1101 Hicks-Jalali, S., R. J. Sica, G. Martucci, E. Maillard Barras, J. Voirin, and A. Haefele (2020). A Raman lidar tropospheric
1102 water vapour climatology and height-resolved trend analysis over Payerne, Switzerland. *Atmos. Chem. Phys.*, **20**(16),
1103 9619–9640.



1104 Huang, G., Liu, X., Chance, K., Yang, K., Bhartia, P. K., Cai, Z., Allaart, M., Ancellet, G., Calpini, B., Coetzee, G. J.
1105 R., Cuevas-Agulló, E., Cupeiro, M., De Backer, H., Dubey, M. K., Fuelberg, H. E., Fujiwara, M., Godin-Beekmann, S.,
1106 Hall, T. J., Johnson, B., Joseph, E., Kivi, R., Kois, B., Komala, N., König-Langlo, G., Laneve, G., Leblanc, T., Marchand,
1107 M., Minschwaner, K. R., Morris, G., Newchurch, M. J., Ogino, S.-Y., Ohkawara, N., Piters, A. J. M., Posny, F., Querel,
1108 R., Scheele, R., Schmidlin, F. J., Schnell, R. C., Schrems, O., Selkirk, H., Shiotani, M., Skriváneková, P., Stübi, R., Taha,
1109 G., Tarasick, D. W., Thompson, A. M., Thouret, V., Tully, M. B., Van Malderen, R., Vömel, H., von der Gathen, P.,
1110 Witte, J. C., and Yela, M.: Validation of 10-year SAO OMI Ozone Profile (PROFOZ) product using ozonesonde
1111 observations, *Atmos. Meas. Tech.*, 10, 2455–2475, <https://doi.org/10.5194/amt-10-2455-2017>, 2017.
1112 Hubert, D., K.-P. Heue, J.-C. Lambert, T. Verhoelst, M. Allaart, S. Compernolle, P. D. Cullis, A. Dehn, C. Félix, B. J.
1113 Johnson, A. Keppens, D. E. Kollonige, C. Lerot, D. Loyola, M. Mohamad, M. Paulete Pereira Martins, A. J. M. Piters,
1114 Selkirk, H. B., A. M. Thompson, P. Veefkind, H. Vömel, J. C. Witte, and C. Zehner (2021). TROPOMI tropospheric
1115 ozone column data : Geophysical assessment and comparison to ozonesondes, GOME-2B and OMI, *Atmos. Meas. Tech.*,
1116 **14**, 7405–7433, <https://doi.org/10.5194/amt-14-7405-2021>
1117 Jalali, A., Walker, K. A., Strong, K., Buchholz, R. R., Deeter, M. N., Wunch, D., Roche, S., Wizenberg, T., Lutsch, E.,
1118 McGee, E., Worden, H. M., Fogal, P., and Drummond, J. R.: A comparison of carbon monoxide retrievals between the
1119 MOPITT satellite and Canadian high-Arctic ground-based NDACC and TCCON FTIR measurements, *Atmos. Meas.
1120 Tech.*, 15, 6837–6863, <https://doi.org/10.5194/amt-15-6837-2022>, 2022.
1121 Johnson, M. S., Philip, S., Meech, S., Kumar, R., Sorek-Hamer, M., Shiga, Y. P., and Jung, J.: Insights into the long-
1122 term (2005–2021) spatiotemporal evolution of summer ozone production sensitivity in the Northern Hemisphere derived
1123 with the Ozone Monitoring Instrument (OMI), *Atmos. Chem. Phys.*, 24, 10363–10384, [https://doi.org/10.5194/acp-24-10363-2024](https://doi.org/10.5194/acp-24-
1124 10363-2024), 2024.
1125 John SS, Deutscher NM, Paton-Walsh C, Velazco VA, Jones NB, Griffith DWT. 2019–20 Australian Bushfires and
1126 Anomalies in Carbon Monoxide Surface and Column Measurements. *Atmosphere*. 2021; 12(6):755.
1127 <https://doi.org/10.3390/atmos12060755>
1128 Johnson, M. S., Liu, X., Zoogman, P., Sullivan, J., Newchurch, M. J., Kuang, S., Leblanc, T., and McGee, T.: Evaluation
1129 of potential sources of a priori ozone profiles for TEMPO tropospheric ozone retrievals, *Atmos. Meas. Tech.*, 11, 3457–
1130 3477, <https://doi.org/10.5194/amt-11-3457-2018>, 2018.
1131 Keppens, A., Di Pede, S., Hubert, D., Lambert, J.-C., Veefkind, P., Sneep, M., De Haan, J., ter Linden, M., Leblanc, T.,
1132 Compernolle, S., Verhoelst, T., Granville, J., Nath, O., Fjaeraa, A. M., Boyd, I., Niemeijer, S., Van Malderen, R., Smit,
1133 H. G. J., Duflat, V., Godin-Beekmann, S., Johnson, B. J., Steinbrecht, W., Tarasick, D. W., Kollonige, D. E., Stauffer,
1134 R. M., Thompson, A. M., Dehn, A., and Zehner, C. (2024). Five years of Sentinel-5p TROPOMI operational ozone
1135 profiling and geophysical validation using ozonesonde and lidar ground-based networks, *Atmos. Meas. Tech.*, **17**, 3969–
1136 3993, <https://doi.org/10.5194/amt-2023-264>
1137 Khaykin, S., Bekki, S., Godin-Beekmann, S., Fromm, M. D., Goloub, P., Hu, Q., Josse, B., Laeng, A., Meziane, M.,
1138 Peterson, D. A., Pelletier, S., and Thouret, V. (2025). Stratospheric impact of the anomalous 2023 Canadian wildfires:
1139 the two vertical pathways of smoke. *Atmos. Chem. Phys.*, **25**, 14551–14571. <https://doi.org/10.5194/acp-25-14551-2025>.
1140 Khaykin, S., Legras, B., Bucci, S. et al. (2020). The 2019/20 Australian wildfires generated a persistent smoke-charged
1141 vortex rising up to 35 km altitude. *Commun Earth Environ* **1**, 22. <https://doi.org/10.1038/s43247-020-00022-5>.



1142 Khaykin, S., Podglajen, A., Ploeger, F. et al. (2022). Global perturbation of stratospheric water and aerosol burden by
1143 Hunga eruption. *Commun Earth Environ* **3**, 316. <https://doi.org/10.1038/s43247-022-00652-x>.

1144 Khaykin, S. M., et al. (2017). Variability and evolution of the midlatitude stratospheric aerosol budget from 22 years of
1145 ground-based lidar and satellite observations. *Atmos. Chem. Phys.*, **17**(3), 1829–1845.

1146 Khaykin, S. M., Hauchecorne, A., Wing, R., Keckhut, P., Godin-Beekmann, S., Porteneuve, J., Mariscal, J.-F., and
1147 Schmitt, J (2020). Doppler lidar at Observatoire de Haute-Provence for wind profiling up to 75 km altitude: performance
1148 evaluation and observations. *Atmos. Meas. Tech.*, **13**, 1501–1516. <https://doi.org/10.5194/amt-13-1501-2020>.

1149 Knepp, T. N., Thomason, L., Roell, M., Damadeo, R., Leavor, K., Leblanc, T., Chouza, F., Khaykin, S., Godin-
1150 Beekmann, S., and Flittner, D.: Evaluation of a method for converting Stratospheric Aerosol and Gas Experiment
1151 (SAGE) extinction coefficients to backscatter coefficients for intercomparison with lidar observations, *Atmos. Meas.*
1152 *Tech.*, **13**, 4261–4276, <https://doi.org/10.5194/amt-13-4261-2020>, 2020.

1153 Kurylo, M. J., Thompson, A. M., and De Mazière, M.: The Network for the Detection of Atmospheric Composition
1154 Change: 25 Years Old and Going Strong, *The Earth Observer*, **28**, 4–15, 2016.

1155 Kwon, H.-A., González Abad, G., Nowlan, C. R., Chong, H., Souri, A. H., Vigouroux, C., Röhling, A., Kivi, R.,
1156 Makarova, M., Notholt, J., Palm, M., Winkler, H., Té, Y., Sussmann, R., Rettinger, M., Mahieu, E., Strong, K., Lutsch,
1157 E., Yamanouchi, S., Nagahama, T., Hannigan, J. W., Zhou, M., Murata, I., Grutter, M., Stremme, W., De Mazière, M.,
1158 Jones, N., Smale, D., Morino, I. (2023). Validation of OMPS Suomi NPP and OMPS NOAA-20 Formaldehyde Total
1159 Columns with NDACC FTIR Observations. *Earth and Space Science*, **10**(5). <https://doi.org/10.1029/2022EA002778>.

1160 Laj, P., and Coauthors, 2024: Aerosol, Clouds and Trace Gases Research Infrastructure (ACTRIS): The European
1161 Research Infrastructure Supporting Atmospheric Science. *Bull. Amer. Meteor. Soc.*, **105**, E1098–E1136,
1162 <https://doi.org/10.1175/BAMS-D-23-0064.1>.

1163 Langerock, B. et al., (2023): Validation Report IASI CO CDR Nov 2025.
1164 https://acsaf.org/docs/vr/Validation_ReportIASI_CO_CDR_Nov_2023.pdf

1165 Langerock, B., et al., (2023): Validation Report IASI HNO3 April 2022,
1166 https://acsaf.org/docs/vr/Validation_ReportIASI_HNO3_Apr_2022.pdf

1167 Laube, J. C., Tegtmeier, S., Fernandez, R. P., Harrison, J., Hu, L., Krummel, P., Mahieu, E., Park, S. and Western, L.
1168 (2022). Update on Ozone-Depleting Substances (ODSs) and Other Gases of Interest to the Montreal Protocol, in
1169 *Scientific Assessment of Ozone Depletion: 2022*, World Meteorological Organization.

1170 Lauther, V., Vogel, B., Wintel, J., Rau, A., Hoor, P., Bense, V., Müller, R., and Volk, C. M. (2022). In situ observations
1171 of CH₂Cl₂ and CHCl₃ show efficient transport pathways for very short-lived species into the lower stratosphere via the
1172 Asian and the North American summer monsoon. *Atmos. Chem. Phys.*, **22**, 2049–2077. <https://doi.org/10.5194/acp-22-2049-2022>.

1173 Leblanc, T., I. S. McDermid, and T. D. Walsh (2012). Ground-based water vapor raman lidar measurements up to the
1175 upper troposphere and lower stratosphere for long-term monitoring. *Atmos. Meas. Tech.*, **5**(1), 17–36.

1176 Lee, G. T., Park, R. J., Kwon, H.-A., Ha, E. S., Lee, S. D., Shin, S., Ahn, M.-H., Kang, M., Choi, Y.-S., Kim, G., Lee,
1177 D.-W., Kim, D.-R., Hong, H., Langerock, B., Vigouroux, C., Lerot, C., Hendrick, F., Pinardi, G., De Smedt, I., Van
1178 Roozendael, M., Wang, P., Chong, H., Cho, Y., and Kim, J. (2024). First evaluation of the GEMS formaldehyde product



1179 against TROPOMI and ground-based column measurements during the in-orbit test period. *Atmos. Chem. Phys.*, **24**,
1180 4733–4749. <https://doi.org/10.5194/acp-24-4733-2024>.

1181 Livesey, N. J., Read, W. G., Froidevaux, L., Lambert, A., Santee, M. L., Schwartz, M. J., Millán, L. F., Jarnot, R. F.,
1182 Wagner, P. A., Hurst, D. F., Walker, K. A., Sheese, P. E., and Nedoluha, G. E.: Investigation and amelioration of long-
1183 term instrumental drifts in water vapor and nitrous oxide measurements from the Aura Microwave Limb Sounder (MLS)
1184 and their implications for studies of variability and trends, *Atmos. Chem. Phys.*, **21**, 15409–15430,
1185 <https://doi.org/10.5194/acp-21-15409-2021>, 2021.

1186 Lutsch, E., Strong, K., Jones, D. B., Ortega, I., Hannigan, J. W., Dammers, E., et al. (2019). Unprecedented atmospheric
1187 ammonia concentrations detected in the high Arctic from the 2017 Canadian wildfires. *Journal of Geophysical Research: Atmospheres*, **124**(14), 8178–8202. <https://doi.org/10.1029/2019jd030419>

1188 Lutsch, E., Wunch, D., Jones, D.B.A., et al. (2022), Can the data assimilation of CO from MOPITT or IASI constrain
1189 high-latitude wildfire emissions? A Case Study of the 2017 Canadian Wildfires. ESS Open Archive, DOI:
1190 10.1002/essoar.10510875.1

1191 Maillard Barras, E., Haefele, A., Stübi, R., Jouberton, A., Schill, H., Petropavlovskikh, I., Miyagawa, K., Stanek, M.,
1192 and Froidevaux, L.: Dynamical linear modeling estimates of long-term ozone trends from homogenized Dobson Umkehr
1193 profiles at Arosa/Davos, Switzerland, *Atmos. Chem. Phys.*, **22**, 14283–14302, <https://doi.org/10.5194/acp-22-14283-2022>, 2022.

1194 Mahieu, E., Chipperfield, M. P., Notholt, J., Redmann, T., Anderson, J., Bernath, P. F., Blumenstock, T., Coffey, M.
1195 T., Dhomse, S. S., Feng, W., Franco, B., Froidevaux, L., Griffith, D. W. T., Hannigan, J. W., Hase, F., Hossaini, R.,
1196 Jones, N. B., Morino, I., Murata, I., Nakajima, H., Palm, M., Paton-Walsh, C., Russell, J. M., Schneider, M., Servais, C.,
1197 Smale, D. and Walker, K. A. (2014). Recent Northern Hemisphere stratospheric HCl increase due to atmospheric
1198 circulation changes. *Nature*, **515**(7525), 104–107. doi:10.1038/nature13857.

1199 Mahieu, E., Fischer, E. V., Franco, B., Palm, M., Wizenberg, T., Smale, D., Clarisse, L., Clerbaux, C., Coheur, P.-F.,
1200 Hannigan, J. W., Lutsch, E., Notholt, J., Cantos, I. P., Prignon, M., Servais, C., and Strong, K. (2021). First retrievals of
1201 peroxyacetyl nitrate (PAN) from ground-based FTIR solar spectra recorded at remote sites, comparison with model and
1202 satellite data. *Elementa: Science of the Anthropocene*, **9**(1), 00027.

1203 Manney, G. L., Livesey, N. J., Santee, M. L., Froidevaux, L., Lambert, A., & Lawrence, Z. D., et al. (2020). Record-low
1204 Arctic stratospheric ozone in 2020: MLS observations of chemical processes and comparisons with previous extreme
1205 winters. *Geophysical Research Letters*, **47**, e2020GL089063. <https://doi.org/10.1029/2020GL089063>

1206 McKenzie, R., Liley, B., Kotkamp, M., Geddes, A., Querel, R., Stierle, S., & Madronich, S. (2022). Relationship between
1207 ozone and biologically relevant UV at 4 NDACC sites. *Photochemical & Photobiological Sciences*, **21**(12), 2095–2114.

1208 McKenzie, R.L., Lucas, R.M. (2018). Reassessing Impacts of Extended Daily Exposure to Low Level Solar UV
1209 Radiation. *Sci Rep* **8**, 13805.

1210 Mettig, N., Weber, M., Rozanov, A., Arosio, C., Burrows, J. P., Veefkind, P., Thompson, A. M., Querel, R., Leblanc,
1211 T., Godin-Beekmann, S., Kivi, R., and Tully, M. B.: Ozone profile retrieval from nadir TROPOMI measurements in the
1212 UV range, *Atmos. Meas. Tech.*, **14**, 6057–6082, <https://doi.org/10.5194/amt-14-6057-2021>, 2021.

1213 Mettig, N., Weber, M., Rozanov, A., Burrows, J. P., Veefkind, P., Thompson, A. M., Stauffer, R. M., Leblanc, T.,
1214 Ancellet, G., Newchurch, M. J., Kuang, S., Kivi, R., Tully, M. B., Van Malderen, R., Piters, A., Kois, B., Stübi, R., and



1217 Skrivankova, P.: Combined UV and IR ozone profile retrieval from TROPOMI and CrIS measurements, *Atmos. Meas.
1218 Tech.*, **15**, 2955–2978, <https://doi.org/10.5194/amt-15-2955-2022>, 2022.

1219 Millán, L. F., Hoor, P., Hegglin, M. I., Manney, G. L., Boenisch, H., Jeffery, P., Kunkel, D., Petropavlovskikh, I., Ye,
1220 H., Leblanc, T., and Walker, K. (2024). Exploring ozone variability in the upper troposphere and lower stratosphere
1221 using dynamical coordinates. *EGUsphere* [preprint]. <https://doi.org/10.5194/egusphere-2024-144>.

1222 Millán, L. F., Santee, M. L., Lambert, A., Livesey, N. J., Werner, F., Schwartz, M. J., Pumphrey, H. C., Manney, G. L.,
1223 Wang, Y., Su, H., Wu, L., Read, W. G., and Froidevaux, L. (2022). The Hunga-Tonga Ha'apai hydration of the
1224 stratosphere. *Geophys. Res. Lett.*, **49**, e2022GL099381. <https://doi.org/10.1029/2022GL099381>.

1225 Millán, L. F., Manney, G. L., Boenisch, H., Hegglin, M. I., Hoor, P., Kunkel, D., Leblanc, T., Petropavlovskikh, I.,
1226 Walker, K., Wargan, K., and Zahn, A. (2023). Multi-parameter dynamical diagnostics for upper tropospheric and lower
1227 stratospheric studies. *Atmos. Meas. Tech.*, **16**, 2957–2988. <https://doi.org/10.5194/amt-16-2957-2023>.

1228 Minganti, D., Chabriat, S., Errera, Q., Prignon, M., Schneider, M., Smale, D., Jones, N. and Mahieu, E. (2022).
1229 Evaluation of the N2O Rate of Change to Understand the Stratospheric Brewer-Dobson Circulation in a Chemistry-
1230 Climate Model. *J. Geophys. Res. Atmos.*, **127**, 1–22. doi:10.1029/2021JD036390.

1231 Molod, A., Takacs, L., Suarez, M., and Bacmeister, J. (2015). Development of the GEOS-5 atmospheric general
1232 circulation model: Evolution from MERRA to MERRA2. *Geoscientific Model Development*, **8**, 1339–1356.
1233 <https://doi.org/10.5194/gmd-8-1339-2015>.

1234 Montzka, S.A., Dutton, G.S., Yu, P. et al. An unexpected and persistent increase in global emissions of ozone-depleting
1235 CFC-11. *Nature* **557**, 413–417 (2018). <https://doi.org/10.1038/s41586-018-0106-2>

1236 Müller, J.-F., Stavrakou, T., Oomen, G.-M., Opacka, B., De Smedt, I., Guenther, A., Vigouroux, C., Langerock, B.,
1237 Aquino, C. A. B., Grutter, M., Hannigan, J., Hase, F., Kivi, R., Lutsch, E., Mahieu, E., Makarova, M., Metzger, J.-M.,
1238 Morino, I., Murata, I., Nagahama, T., Notholt, J., Ortega, I., Palm, M., Röhling, A., Stremme, W., Strong, K., Sussmann,
1239 R., Té, Y., and Fried, A. (2024). Bias correction of OMI HCHO columns based on FTIR and aircraft measurements and
1240 impact on top-down emission estimates. *Atmos. Chem. Phys.*, **24**, 2207–2237. <https://doi.org/10.5194/acp-24-2207-2024>.

1241 Navas-Guzmán, F., Kämpfer, N., Schranz, F., Steinbrecht, W., and Haefele, A.: Intercomparison of stratospheric
1242 temperature profiles from a ground-based microwave radiometer with other techniques, *Atmos. Chem. Phys.*, **17**, 14085–
1243 14104, <https://doi.org/10.5194/acp-17-14085-2017>, 2017.

1244 Nedoluha, G. E., Gomez, R. M., Boyd, I., Neal, H., Allen, D. R., and Lambert, A. (2024). The spread of the Hunga Tonga
1245 H2O plume in the middle atmosphere over the first two years since eruption. *Journal of Geophysical Research: Atmospheres*, **129**(11):e2024JD040907.

1246 Nedoluha, G. E., Gomez, R. M., Boyd, I., Neal, H., Allen, D. R., Lambert, A., and Livesey, N. J. (2023). Mesospheric
1247 Water Vapor in 2022. *Journal of Geophysical Research: Atmospheres*, **128**(18):e2023JD039196.

1248 Nedoluha, G. E., Gomez, R. M., Boyd, I., Neal, H., Allen, D. R., Lambert, A., and Livesey, N. J. (2023). Measurements
1249 of Stratospheric Water Vapor at Mauna Loa and the Effect of the Hunga Tonga Eruption. *Journal of Geophysical
1250 Research: Atmospheres*, **128**(8):e2022JD038100.

1251 Nedoluha, G. E., Kiefer, M., Lossow, S., Gomez, R. M., Kämpfer, N., Lainer, M., Forkman, P., Christensen, O. M., Oh,
1252 J. J., Hartogh, P., Anderson, J., Bramstedt, K., Dinelli, B. M., Garcia-Comas, M., Hervig, M., Murtagh, D., Raspollini,
1253 P., Read, W. G., Rosenlof, K., Stiller, G. P., and Walker, K. A. (2017). The Sparc water vapor assessment ii:
1254



1255 intercomparison of satellite and ground-based microwave measurements. *Atmospheric Chemistry and Physics*,
1256 **17**(23):14543–14558.

1257 Nielsen, J. E., Pawson, S., Molod, A., Auer, B., da Silva, A. M., Douglass, A. R., et al. (2017). Chemical mechanisms
1258 and their applications in the Goddard Earth Observing System (GEOS) earth system model. *Journal of Advances in*
1259 *Modeling Earth Systems*, **9**, 3019–3044. <https://doi.org/10.1002/2017MS001011>.

1260 Oomen, G.-M., Müller, J.-F., Stavrakou, T., De Smedt, I., Blumenstock, T., Kivi, R., Makarova, M., Palm, M., Röhling,
1261 A., Té, Y., Vigouroux, C., Friedrich, M. M., Frieß, U., Hendrick, F., Merlaud, A., Piters, A., Richter, A., Van Roozendael,
1262 M., and Wagner, T. (2024). Weekly derived top-down volatile-organic-compound fluxes over Europe from TROPOMI
1263 HCHO data from 2018 to 2021. *Atmos. Chem. Phys.*, **24**, 449–474. <https://doi.org/10.5194/acp-24-449-2024>.

1264 Orbe, C., Oman, L. D., Strahan, S. E., Waugh, D. W., Pawson, S., Takacs, L. L., & Molod, A. M. (2017). Large-scale
1265 atmospheric transport in GEOS replay simulations. *Journal of Advances in Modeling Earth Systems*, **9**, 2545–2560.
1266 <https://doi.org/10.1002/2017MS001053>.

1267 Orbe, C., Plummer, D. A., Waugh, D. W., Yang, H., Jöckel, P., Kinnison, D. E., Josse, B., Marecal, V., Deushi, M.,
1268 Abraham, N. L., Archibald, A. T., Chipperfield, M. P., Dhomse, S., Feng, W., and Bekki, S.: Description and Evaluation
1269 of the specified-dynamics experiment in the Chemistry-Climate Model Initiative , *Atmos. Chem. Phys.*, **20**, 3809–3840,
1270 <https://doi.org/10.5194/acp-20-3809-2020>, 2020.

1271 Orphal, J., Staehelin, J., Tamminen, J., Braathen, G., De Backer, M.-R., Bais, A., Balis, D., Barbe, A., Bhartia, P. K.,
1272 Birk, M., Burkholder, J. B., Chance, K., von Clarmann, T., Cox, A., Degenstein, D., Evans, R., Flaud, J.-M., Flittner, D.,
1273 Godin-Beekmann, S., Gorshelev, V., Gratien, A., Hare, E., Janssen, C., Kyrölä, E., McElroy, T., McPeters, R., Pastel,
1274 M., Petersen, M., Petropavlovskikh, I., Picquet-Varrault, B., Pitts, M., Labow, G., Rotger-Languereau, M., Leblanc, T.,
1275 Lerot, C., Liu, X., Moussay, P., Redondas, A., Van Roozendael, M., Sander, S. P., Schneider, M., Serdyuchenko, A.,
1276 Veefkind, P., Viallon, J., Viatte, C., Wagner, G., Weber, M., Wielgosz, R. I., and Zehner, C. (2016). Absorption cross-
1277 sections of ozone in the ultraviolet and visible spectral regions: Status report 2015. *J. Mol. Spectrosc.*, **327**, 105–121.
1278 <https://doi.org/10.1016/j.jms.2016.07.007>.

1279 Pan, L. L. (Corresponding author) ; Atlas, E. L. ; Honomichl, S. B. ; Smith, W. P. ; Kinnison, D. E. ; Solomon, S. ;
1280 Santee, M. L. ; Saiz-Lopez, A. ; Laube, J. C. ; Wang, B. ; Ueyama, R. ; Bresch, J. F. ; Hornbrook, R. S. ; Apel, E. C. ;
1281 Hills, A. J. ; Treadaway, V. ; Smith, K. ; Schaufler, S. ; Donnelly, S. ; Hendershot, R. ; Lueb, R. ; Campos, T. ; Viciani,
1282 S. ; D'Amato, F. ; Bianchini, G. ; Barucci, M. ; Podolske, J. R. ; Iraci, L. T. ; Gurganus, C. ; Bui, P. ; Dean-Day, J. M. ;
1283 Millán, L. ; Ryoo, J.-M. ; Barletta, B. ; Koo, J.-H. ; Kim, J. ; Liang, Q. ; Randel, W. J. ; Thornberry, T. ; Newman, P. A.
1284 (2022): East Asian summer monsoon delivers large abundances of very short-lived organic chlorine substances to the
1285 lower stratosphere, *P. Natl. Acad. Sci.*, **119**(25), e2117325119, 2022.

1286 Pardo Cantos, I., Mahieu, E., Chipperfield, M. P., Smale, D., Hannigan, J. W., Friedrich, M., Fraser, P., Krummel, P.,
1287 Prignon, M., Makkor, J., Servais, C. and Robinson, J. (2022). Determination and analysis of time series of CFC-11
1288 (CCl₃F) from FTIR solar spectra, in situ observations, and model data in the past 20 years above Jungfraujoch (46°N),
1289 Lauder (45°S), and Cape Grim (40°S) stations. *Environ. Sci. Atmos.*, doi:10.1039/D2EA00060A.

1290 Pardo Cantos, I., Mahieu, E., Chipperfield, M.P., Servais, C., Reimann, S., Vollmer, M.K. (2024). First HFC-134a
1291 retrievals from ground-based FTIR solar absorption spectra, comparison with TOMCAT model simulations, in-situ



1292 AGAGE observations, and ACE-FTS satellite data for the Jungfraujoch station. *Journal of Quantitative Spectroscopy*
1293 and Radiative Transfer

, **318**, 108938. <https://doi.org/10.1016/j.jqsrt.2024.108938>.

1294 Pazmiño, A., Goutail, F., Godin-Beekmann, S., Hauchecorne, A., Pommereau, J.-P., Chipperfield, M. P., Feng, W.,
1295 Lefèvre, F., Lecouffe, A., Van Roozendael, M., Jepsen, N., Hansen, G., Kivi, R., Strong, K., and Walker, K. A.: Trends
1296 in polar ozone loss since 1989: potential sign of recovery in the Arctic ozone column, *Atmos. Chem. Phys.*, **23**, 15655–
1297 15670, <https://doi.org/10.5194/acp-23-15655-2023>, 2023.

1298 Peterson, D. A., and Coauthors, 2022: Measurements from inside a Thunderstorm Driven by Wildfire: The 2019 FIREX-
1299 AQ Field Experiment. *Bull. Amer. Meteor. Soc.*, **103**, E2140–E2167, <https://doi.org/10.1175/BAMS-D-21-0049.1>.

1300 Petropavlovskikh, I., Wild, J. D., Abromitis, K., Effertz, P., Miyagawa, K., Flynn, L. E., Maillard Barras, E., Damadeo,
1301 R., McConville, G., Johnson, B., Cullis, P., Godin-Beekmann, S., Ancellet, G., Querel, R., Van Malderen, R., and
1302 Zawada, D.: Ozone trends in homogenized Umkehr, ozonesonde, and COH overpass records, *Atmos. Chem. Phys.*, **25**,
1303 2895–2936, <https://doi.org/10.5194/acp-25-2895-2025>, 2025.

1304 Pinardi, G., Van Roozendael, M., Hendrick, F., Richter, A., Valks, P., Alwarda, R., Bognar, K., Frieß, U., Granville, J.,
1305 Gu, M., Johnston, P., Prados-Roman, C., Querel, R., Strong, K., Wagner, T., Wittrock, F., and Yela Gonzalez, M.:
1306 Ground-based validation of the MetOp-A and MetOp-B GOME-2 OCIO measurements, *Atmos. Meas. Tech.*, **15**, 3439–
1307 3463, <https://doi.org/10.5194/amt-15-3439-2022>, 2022.

1308 Ploeger, F., Diallo, M., Charlesworth, E., Konopka, P., Legras, B., Laube, J. C., Grooß, J.-U., Günther, G., Engel, A.,
1309 and Riese, M.: The stratospheric Brewer–Dobson circulation inferred from age of air in the ERA5 reanalysis, *Atmos.*
1310 *Chem. Phys.*, **21**, 8393–8412, <https://doi.org/10.5194/acp-21-8393-2021>, 2021.

1311 Polyakov, A., Poberovsky, A., Makarova, M., Virolainen, Y., Timofeyev, Y., and Nikulina, A. (2021). Measurements of
1312 CFC-11, CFC-12, and HCFC-22 total columns in the atmosphere at the St. Petersburg site in 2009–2019. *Atmospheric*
1313 *Measurement Techniques*, **14**(8):5349–5368.

1314 Pommrich, R., Müller, R., Grooß, J.-U., Konopka, P., Ploeger, F., Vogel, B., Tao, M., Hoppe, C. M., Günther, G., Spelten,
1315 N., Hoffmann, L., Pumphrey, H.-C., Viciani, S., D’Amato, F., Volk, C. M., Hoor, P., Schlager, H., and Riese, M.:
1316 Tropical troposphere to stratosphere transport of carbon monoxide and long-lived trace species in the Chemical
1317 Lagrangian Model of the Stratosphere (CLaMS), *Geosci. Model Dev.*, **7**, 2895–2916,
1318 <https://doi.org/10.5194/gmd-7-2895-2014>, 2014.

1319 Prignon, M., Chabriat, S., Friedrich, M., Smale, D., Strahan, S. E., Bernath, P. F., Chipperfield, M. P., Dhomse, S. S.,
1320 Feng, W., Minganti, D., Servais, C. and Mahieu, E. (2021). Stratospheric fluorine as a tracer of circulation changes:
1321 comparison between infrared remote-sensing observations and simulations with five modern reanalyses. *J. Geophys. Res.*
1322 *Atmos.*, doi:10.1029/2021JD034995.

1323 Ratynski, M., Khaykin, S., Hauchecorne, A., Wing, R., Cammas, J.-P., Hello, Y., and Keckhut, P. (2023). Validation of
1324 Aeolus wind profiles using ground-based lidar and radiosonde observations at Réunion island and the Observatoire de
1325 Haute-Provence. *Atmos. Meas. Tech.*, **16**, 997–1016. <https://doi.org/10.5194/amt-16-997-2023>.

1326 Read, W. G., Stiller, G., Lossow, S., Kiefer, M., Khosrawi, F., Hurst, D., Vömel, H., Rosenlof, K., Dinelli, B. M.,
1327 Raspollini, P., Nedoluha, G. E., Gille, J. C., Kasai, Y., Eriksson, P., Sioris, C. E., Walker, K. A., Weigel, K., Burrows, J.
1328 P., and Rozanov, A.: The SPARC Water Vapor Assessment II: assessment of satellite measurements of upper
1329 tropospheric humidity, *Atmos. Meas. Tech.*, **15**, 3377–3400, <https://doi.org/10.5194/amt-15-3377-2022>, 2022.



1330 Redondas, A. et al (2024), WMO (World Meteorological Organization) (2024): Eighteenth Intercomparison Campaign
1331 of the Regional Brewer Calibration Centre Europe, El Arenosillo Atmospheric Sounding Station, Huelva, Spain, 4–15
1332 September 2023, GAW Report No. 302, 81 pp., WMO, Geneva, <https://doi.org/10.31978/666-20-018-3>

1333 Rennie, M.P., Isaksen, L., Weiler, F., de Kloet, J., Kanitz, T. & Reitebuch, O. (2021). The impact of Aeolus wind retrievals
1334 on ECMWF global weather forecasts. *Q J R Meteorol Soc*, **147**(740), 3555–3586. <https://doi.org/10.1002/qj.4142>.

1335 Salawitch, R. J., J. B. Smith, H. B. Selkirk, K. Wargan, M. Chipperfield, R. Hossaini, P. Levelt, N. Livesey, L. McBride,
1336 L. Millán, E. Moyer, M. Santee, M. R. Schoeberl, S. Solomon, K. Stone and H. Worden (2025). The Imminent Data
1337 Desert: The future of stratospheric monitoring in a rapidly changing world. *Bull. Amer. Meteor. Soc.*
1338 <https://doi.org/10.1175/BAMS-D-23-0281.1>.

1339 Santee, M. L., Lambert, A., Manney, G. L., Livesey, N. J., Froidevaux, L., Neu, J. L., et al. (2022). Prolonged and
1340 pervasive perturbations in the composition of the Southern Hemisphere midlatitude lower stratosphere from the
1341 Australian New Year's fires. *Geophysical Research Letters*, **49**, e2021GL096270.
1342 <https://doi.org/10.1029/2021GL096270>.

1343 Sauvageat, E., Maillard Barras, E., Hocke, K., Haefele, A., and Murk, A.: Harmonized retrieval of middle atmospheric
1344 ozone from two microwave radiometers in Switzerland, *Atmos. Meas. Tech.*, **15**, 6395–6417,
1345 <https://doi.org/10.5194/amt-15-6395-2022>, 2022.

1346 Serdyuchenko, A., Gorshelev, V., Weber, M., Chehade, W., and Burrows, J. P. (2014). High spectral resolution ozone
1347 absorption cross-sections – Part 2: Temperature dependence. *Atmos. Meas. Tech.*, **7**, 625–636.
1348 <https://doi.org/10.5194/amt-7-625-2014> (data available at: <https://www.iup.unibremen.de/gruppen/molspec/databases/referencespectra/o3spectra2011/index.html>, last access: 11 April 2024).

1349 Sha, M. K., De Mazière, M., Notholt, J., Blumenstock, T., Chen, H., Dehn, A., Griffith, D. W. T., Hase, F., Heikkinen,
1350 P., Hermans, C., Hoffmann, A., Huebner, M., Jones, N., Kivi, R., Langerock, B., Petri, C., Scolas, F., Tu, Q., and
1351 Weidmann, D. (2020). Intercomparison of low- and high-resolution infrared spectrometers for ground-based solar remote
1352 sensing measurements of total column concentrations of CO₂, CH₄, and CO. *Atmos. Meas. Tech.*, **13**, 4791–4839.
1353 <https://doi.org/10.5194/amt-13-4791-2020>.

1354 Shi, G., Krochin, W., Sauvageat, E., and Stober, G.: Ozone and water vapor variability in the polar middle atmosphere
1355 observed with ground-based microwave radiometers, *Atmos. Chem. Phys.*, **23**, 9137–9159, <https://doi.org/10.5194/acp-23-9137-2023>, 2023

1356 Smit, H. G. J., Poyraz, D., Van Malderen, R., Thompson, A. M., Tarasick, D. W., Stauffer, R. M., Johnson, B. J., and
1357 Kollonige, D. E. (2024). New insights from the Jülich Ozone Sonde Intercomparison Experiment: calibration functions
1358 traceable to one ozone reference instrument. *Atmos. Meas. Tech.*, **17**, 73–112. <https://doi.org/10.5194/amt-17-73-2024>.

1359 Smit, H.G.J., Thompson, A. M., and ASOPOS panel. (2021): Ozonesonde Measurement Principles and Best Operational
1360 Practices, ASOPOS (Assessment of Standard Operating Procedures for Ozonesondes) 2.0, WMO Global Atmosphere
1361 Watch report series, No. 268, World Meteorological Organization, Geneva.
1362 https://library.wmo.int/index.php?lvl=notice_display&id=21986#YaFNSbpOlc8.

1363 Solomon, S., K. Dube, K. Stone, D. Degenstein (2022). On the stratospheric chemistry of midlatitude wildfire smoke.
1364 *Proc. Nat. Acad. Sci.*, **119**, e2117325119. <https://doi.org/10.1073/pnas.2117325119>.



1367 Solomon, S., Stone, K., Yu, P. et al. (2023). Chlorine activation and enhanced ozone depletion induced by wildfire
1368 aerosol. *Nature* **615**, 259–264. <https://doi.org/10.1038/s41586-022-05683-0>.

1369 Souri, A. H., Johnson, M. S., Wolfe, G. M., Crawford, J. H., Fried, A., Wisthaler, A., Brune, W. H., Blake, D. R.,
1370 Weinheimer, A. J., Verhoelst, T., Compernolle, S., Pinardi, G., Vigouroux, C., Langerock, B., Choi, S., Lamsal, L., Zhu,
1371 L., Sun, S., Cohen, R. C., Min, K.-E., Cho, C., Philip, S., Liu, X., and Chance, K. (2023). Characterization of Errors in
1372 Satellite-based HCHO / NO₂ Tropospheric Column Ratios with Respect to Chemistry, Column to PBL Translation,
1373 Spatial Representation, and Retrieval Uncertainties. *Atmos. Chem. Phys.*, **23**, 1963–1986. <https://doi.org/10.5194/acp-23-1963-2023>.

1375 SPARC Report on the Mystery of Carbon Tetrachloride. Q. Liang, P.A. Newman, S. Reimann (Eds.). (2016). SPARC
1376 Report No. 7, WCRP-13/2016. doi: 10.3929/ethz-a-010690647.

1377 Stauffer, R. M., Thompson, A. M., Kollonige, D. E., Witte, J. C., Tarasick, D. W., Davies, J. M., Vömel, H., Morris, G.A.,
1378 Van Malderen, R., Johnson, B. J., Querel, R. R., Selkirk, H. B., Stübi, R., and Smit, H.G.J., et al. (2020). A post-2013 drop-off in total
1379 ozone at third of global ozonesonde stations: ECC Instrument Artifacts?, *Geophys. Res. Lett.*, doi:
1380 10.1029/2019/GL086791, 2020.

1381 Stauffer, R. M., Thompson, A. M., Kollonige, D. E., Tarasick, D. W., Van Malderen, R., Smit, H. G. J., et al. (2022). An
1382 examination of the recent stability of ozonesonde global network data. *Earth and Space Science*, **9**, e2022EA002459.
1383 <https://doi.org/10.1029/2022EA002459>.

1384 Stenke, A., Grewe, V. & Ponater, M. (2007). Lagrangian transport of water vapor and cloud water in the ECHAM4 GCM
1385 and its impact on the cold bias. *Clim. Dyn.* **31**, 491–506.

1386 Strahan, S. E., A. R. Douglass, and P. A. Newman (2013). The contributions of chemistry and transport to low arctic
1387 ozone in March 2011 derived from Aura MLS observations. *J. Geophys. Res. Atmos.*, **118**, 1563–1576.
1388 doi:10.1002/jgrd.50181.

1389 Strahan, S. E., Smale, D., Douglass, A. R., Blumenstock, T., Hannigan, J. W., Hase, F., et al. (2020). Observed
1390 hemispheric asymmetry in stratospheric transport trends from 1994 to 2018. *Geophysical Research Letters*, **47**,
1391 e2020GL088567. <https://doi.org/10.1029/2020GL088567>

1392 Strahan, S. E., Smale, D., Solomon, S., Taha, G., Damon, M. R., Steenrod, S. D., et al. (2022). Unexpected repartitioning
1393 of stratospheric inorganic chlorine after the 2020 Australian wildfires. *Geophysical Research Letters*, **49**,
1394 e2022GL098290. <https://doi.org/10.1029/2022GL098290>.

1395 Takeda, M., Nakajima, H., Murata, I., Nagahama, T., Morino, I., Toon, G. C., Weiss, R. F., Mühle, J., Krummel, P. B.,
1396 Fraser, P. J., and Wang, H.-J.: First ground-based Fourier transform infrared (FTIR) spectrometer observations of HFC-
1397 23 at Rikubetsu, Japan, and Syowa Station, Antarctica, *Atmos. Meas. Tech.*, **14**, 5955–5976, <https://doi.org/10.5194/amt-14-5955-2021>, 2021.

1399 Tarasick, D., I.E. Galbally, et al. (2019). Tropospheric Ozone Assessment Report: Tropospheric ozone from 1877 to
1400 2016, observed levels, trends and uncertainties. *Elem. Sci. Anth.*, **7**:39. doi: <https://doi.org/10.1525/elementa.376>.

1401 Thompson, A.M., Smit, H. G. J., Witte, J. C., Stauffer, R. M. et al: Ozonesonde Quality Assurance: The JOSIE-SHADOZ
1402 (2017) Experience, *Bull. Am. Meteor. Society*, doi.org/10.1175/BAMS-D-17-0311.1, 2019

1403 Thompson, A. M., Stauffer, R. M., Kollonige, D. E., Ziemke, J. R., Johnson, B. J., Morris, G. A., Cullis P., Cazorla, M.,
1404 Diaz, J. A., Piters, A., Nedeljkovic, I., Warsidikromo, T., Silva, F. R., Northam, E. T., Benjamin, P., Mkololo, T.,



1405 Machinini, T., Félix, C., Romanens, G., Nyadida, S., Brioude, J., Evan, S., Metzger, J.-M., Dindang, A., Mahat, Y. B.,
1406 Sammathuria, M. K., Zakaria, N. B., Komala, N., Ogino, S.-Y., Quyen, N. T., Mani, F. S., Vuiyasawa, M., Nardini, D.,
1407 Martinsen, M., Kuniyuki, D. T., Müller, K., Wolff, P., Sauvage, B.: Tropical tropospheric ozone trends (1998 to 2023):
1408 New perspectives from SHADOZ, IAGOS and OMI/MLS observations, *Atmos. Chem. Phys.*, 25, 18475–18507, 2025
1409 Trickl, T., Vogelmann, H., Fromm, M. D., Jäger, H., Perfahl, M., and Steinbrecht, W.: Measurement report: Violent
1410 biomass burning and volcanic eruptions – a new period of elevated stratospheric aerosol over central Europe (2017 to
1411 2023) in a long series of observations, *Atmos. Chem. Phys.*, 24, 1997–2021, <https://doi.org/10.5194/acp-24-1997-2024>,
1412 2024.

1413 Van Malderen, R., Thompson, A. M., Kollonige, D. E., Stauffer, R. M., Smit, H. G. J., Maillard Barras, E., Vigouroux,
1414 C., Petropavlovskikh, I., Leblanc, T., Thouret, V., Wolff, P., Effertz, P., Tarasick, D. W., Poyraz, D., Ancellet, G., De
1415 Backer, M.-R., Evan, S., Flood, V., Frey, M. M., Hannigan, J. W., Hernandez, J. L., Iarlöri, M., Johnson, B. J., Jones,
1416 N., Kivi, R., Mahieu, E., McConville, G., Müller, K., Nagahama, T., Notholt, J., Piters, A., Prats, N., Querel, R., Smale,
1417 D., Steinbrecht, W., Strong, K., and Sussmann, R. (2025a). Global ground-based tropospheric ozone measurements:
1418 reference data and individual site trends (2000–2022) from the TOAR-II/HEGIFTOM project. *Atmos. Chem. Phys.*, 25,
1419 7187–7225. <https://doi.org/10.5194/acp-25-7187-2025>.

1420 Van Malderen, R., Zang, Z., Chang, K.-L., Björklund, R., Cooper, O. R., Liu, J., Maillard Barras, E., Vigouroux, C.,
1421 Petropavlovskikh, I., Leblanc, T., Thouret, V., Wolff, P., Effertz, P., Gaudel, A., Tarasick, D. W., Smit, H. G. J.,
1422 Thompson, A. M., Stauffer, R. M., Kollonige, D. E., Poyraz, D., Ancellet, G., De Backer, M.-R., Frey, M. M., Hannigan,
1423 J. W., Hernandez, J. L., Johnson, B. J., Jones, N., Kivi, R., Mahieu, E., Morino, I., McConville, G., Müller, K., Murata,
1424 I., Notholt, J., Piters, A., Prignon, M., Querel, R., Rizi, V., Smale, D., Steinbrecht, W., Strong, K., and Sussmann, R.
1425 (2025b). Ground-based tropospheric ozone measurements: regional tropospheric ozone column trends from the TOAR-
1426 II/HEGIFTOM homogenized datasets. *Atmos. Chem. Phys.*, 25, 9905–9935. <https://doi.org/10.5194/acp-25-9905-2025>.

1427 Vandenbussche, S.; Langerock, B.; Vigouroux, C.; Buschmann, M.; Deutscher, N.M.; Feist, D.G.; García, O.; Hannigan,
1428 J.W.; Hase, F.; Kivi, R.; Kumps, N.; Makarova, M.; Millet, D.B.; Morino, I.; Nagahama, T.; Notholt, J.; Ohyama, H.;
1429 Ortega, I.; Petri, C.; Rettinger, M.; Schneider, M.; Servais, C.P.; Sha, M.K.; Shiomi, K.; Smale, D.; Strong, K.; Sussmann,
1430 R.; Té, Y.; Velazco, V.A.; Vrekoussis, M.; Warneke, T.; Wells, K.C.; Wunch, D.; Zhou, M.; De Mazière, M. (2022).
1431 Nitrous Oxide Profiling from Infrared Radiances (NOPIR): Algorithm Description, Application to 10 Years of IASI
1432 Observations and Quality Assessment. *Remote Sens.*, 14, 1810. <https://doi.org/10.3390/rs14081810>.

1433 Verhoelst, T., Compernolle, S., Pinardi, G., Lambert, J.-C., Eskes, H. J., Eichmann, K.-U., Fjæraa, A. M., Granville, J.,
1434 Niemeijer, S., Cede, A., Tiefengraber, M., Hendrick, F., Pazmiño, A., Bais, A., Bazzureau, A., Boersma, K. F., Bognar,
1435 K., Dehn, A., Donner, S., Elokhov, A., Gebetsberger, M., Goutail, F., Grutter de la Mora, M., Gruzdev, A., Gratsea, M.,
1436 Hansen, G. H., Irie, H., Jepsen, N., Kanaya, Y., Karagkiozidis, D., Kivi, R., Kreher, K., Levelt, P. F., Liu, C., Müller,
1437 M., Navarro Comas, M., Piters, A. J. M., Pommereau, J.-P., Portafaix, T., Prados-Roman, C., Puentedura, O., Querel,
1438 R., Remmers, J., Richter, A., Rimmer, J., Rivera Cárdenas, C., Saavedra de Miguel, L., Sinyakov, V. P., Stremme, W.,
1439 Strong, K., Van Roozendael, M., Veefkind, J. P., Wagner, T., Wittrock, F., Yela González, M., and Zehner, C. (2021).
1440 Ground-based validation of the Copernicus Sentinel-5P TROPOMI NO₂ measurements with the NDACC ZSL-DOAS,
1441 MAX-DOAS and Pandonia global networks. *Atmos. Meas. Tech.*, 14, 481–510. <https://doi.org/10.5194/amt-14-481-2021>.



1443 Vigouroux, C., C. A. B. Aquino, M. Bauwens, C. Becker, T. Blumenstock, M. D. Mazi`ere, O. Garc`ia, M. Grutter, C.
1444 Guarin, J. W. Hannigan, F. Hase, N. Jones, R. Kivi, D. Koshelev, B. Langerock, E. Lutsch, M. Makarova, J.-M. Metzger,
1445 J.-F. Muller, J. Notholt, I. Ortega, M. Palm, C. Paton-Walsh, A. Poberovskii, M. Rettinger, J. Robinson, D. Smale, T.
1446 Stavrakou, W. Stremme, K. Strong, R. Suss- mann, Y. T`e, and G. Toon. (2018). NDACC harmonized formaldehyde
1447 time-series from 21 FTIR stations covering a wide range of column abundances. *Atmospheric Measurement Techniques*,
1448 **11**(9):5049–5073.

1449 Vigouroux, C., B. Langerock, C. A. Bauer Aquino, T. Blumenstock, Z. Cheng, M. De Mazi`ere, I. De Smedt, M. Grutter,
1450 J. W. Hannigan, N. Jones, R. Kivi, D. Loyola, E. Lutsch, E. Mahieu, M. Makarova, J.-M. Metzger, I. Morino, I. Murata,
1451 T. Nagahama, J. Notholt, I. Ortega, M. Palm, G. Pinardi, A. R`ohling, D. Smale, W. Stremme, K. Strong, R. Sussmann,
1452 Y. T`e, M. van Roozendael, P. Wang, and H. Winkler. (2020). Tropomi–sentinel-5 precursor formaldehyde validation
1453 using an exten- sive network of ground-based fourier-transform infrared stations. *Atmospheric Measurement Techniques*,
1454 **13**(7):3751–3767.

1455 Vogel, B., Volk, C. M., Wintel, J., Lauther, V., Müller, R., Patra, P. K., Riese, M., Terao, Y., and Stroh, F. (2023).
1456 Reconstructing high-resolution in-situ vertical carbon dioxide profiles in the sparsely monitored Asian monsoon region.
1457 *Commun Earth Environ*, **4**. <https://doi.org/10.1038/s43247-023-00725-5>.

1458 Vogel, B., Lauther, V., Kollner, F., Ekinci, F., Rolf, C., Strobel, J., van Luijt, R., Volk, M. C., Borrman, S., Dragoneas,
1459 A., Eppers, O., Molleker, S., Hoor, P., Ort, L., Weyland, F., Zahn, A., Clemens, J., Günther, G., Kachula, O., Müller, R.,
1460 Ploeger, F., and Riese, M.: Continental and marine source regions contributing to the out- flow of the Asian summer
1461 monsoon anticyclone during the PHILEAS campaign in summer 2023, EGUsphere, 2025, 1–49, <https://doi.org/10.5194/egusphere-2025-5609>, URL <https://egusphere.copernicus.org/preprints/2025/egusphere-2025-5609/>, 2025

1462 Voglmeier, K., Velazco, V. A., Egli, L., Gröbner, J., Redondas, A., and Steinbrecht, W. (2024). The transition to new
1463 ozone absorption cross sections for Dobson and Brewer total ozone measurements. *Atmos. Meas. Tech.*, **17**, 2277–2294.
1464 <https://doi.org/10.5194/amt-17-2277-2024>.

1465 Vömel, H., Evan, S., and Tully, M. (2022). Water vapor injection into the stratosphere by Hunga Tonga-Hunga Ha`apai.
1466 *Science*, **377**(6613):1444–1447. doi:10.1126/science.abq2299.

1467 Vömel, H., Naebert, T., Dirksen, R., and Sommer, M. (2016). An update on the uncertainties of water vapor
1468 measurements using cryogenic frost point hygrometers. *Atmos. Meas. Tech.*, **9**, 3755–3768. <https://doi.org/10.5194/amt-9-3755-2016>.

1469 Wang J, Zhou M, Langerock B, Nan W, Wang T, Wang P. (2024). Optimizing the Atmospheric CO₂ Retrieval Based
1470 on the NDACC-Type FTIR Mid-Infrared Spectra at Xianghe, China. *Remote Sensing*. **16**(5):900.
1471 <https://doi.org/10.3390/rs16050900>.

1472 Wang, H. J. R., Damadeo, R., Flittner, D., Kramarova, N., Taha, G., Davis, S., et al. (2020). Validation of SAGE III/ISS
1473 solar occultation ozone products with correlative satellite and ground based measurements. *Journal of Geophysical
1474 Research: Atmospheres*, **125**, e2020JD032430. <https://doi.org/10.1029/2020JD032430>.

1475 Annette Wagner, Y. Bennouna, A.-M. Blechschmidt, G. Brasseur, S. Chabillat, Y. Christophe, Q. Errera, H. Eskes, J.
1476 Flemming, K. M. Hansen, A. Inness, J. Kapsomenakis, B. Langerock, A. Richter, N. Sudarchikova, V. Thouret, C.
1477 Zerefos; Comprehensive evaluation of the Copernicus Atmosphere Monitoring Service (CAMS) reanalysis against



1480 independent observations: Reactive gases. *Elementa: Science of the Anthropocene* 21 January 2021; 9 (1): 00171. doi:
1481 <https://doi.org/10.1525/elementa.2020.00171>

1482 Weber, M., Gorshelev, V., and Serdyuchenko, A. (2016). Uncertainty budgets of major ozone absorption cross sections
1483 used in UV remote sensing applications. *Atmos. Meas. Tech.*, **9**, 4459–4470. <https://doi.org/10.5194/amt-9-4459-2016>
1484 (data available at: <https://www.iup.uni-bremen.de/UVSAT/data/xsectionuncertainty/>, last access: 11 April 2024).

1485 Wells, K. C., Millet, D. B., Payne, V. H., Vigouroux, C., Aquino, C. A. B., De Mazière, M., et al. (2022). Next-generation
1486 isoprene measurements from space: Detecting daily variability at high resolution. *Journal of Geophysical Research: Atmospheres*, **127**, e2021JD036181. <https://doi.org/10.1029/2021JD036181>.

1487 Wells, K., Millet, D., Brewer, J., Payne, V., Cady-Pereira, K., Pernak, R., Kulawick, S., Vigouroux, C., Jones, N.,
1488 Mahieu, E., Makarova, M., Nagahama, T., Ortega, I., Palm, M., Strong, K., Schneider, M., Smale, D., Sussmann, R., and
1489 Zhou, M. (2024). Long-term global measurements of methanol, ethene, ethyne, and HCN from the Cross-track Infrared
1490 Sounder. *EGUsphere* [preprint]. <https://doi.org/10.5194/egusphere-2024-1551>.

1491 Wizenberg, T., Strong, K., Jones, D., Lutsch, E., Mahieu, E., Franco, B., & Clarisse, L. (2022). Replication data for:
1492 Exceptional wildfire enhancements of PAN, C2H4, CH3OH, and HCOOH over the Canadian high Arctic during August
1493 2017 [Dataset]. Borealis. <https://doi.org/10.5683/SP3/6PBAHK>

1494 Wizenberg, T., Strong, K., Jones, D. B. A., Lutsch, E., Mahieu, E., Franco, B., & Clarisse, L. (2023). Exceptional wildfire
1495 enhancements of PAN, C2H4, CH3OH, and HCOOH over the Canadian high Arctic during August 2017. *Journal of Geophysical Research: Atmospheres*, **128**, e2022JD038052. <https://doi.org/10.1029/2022JD038052>.

1496 WMO (World Meteorological Organization). (2014). **Scientific Assessment of Ozone Depletion: 2014**. Global Ozone
1497 Research and Monitoring Project-Report No. 55, 416 pp., Geneva, Switzerland.
1498 <https://www.csl.noaa.gov/assessments/ozone/2014/>.

1499 WMO (World Meteorological Organization). (2022). **Scientific Assessment of Ozone Depletion: 2022**. GAW Report
1500 No. 278, 509 pp., WMO, Geneva, Switzerland. <https://www.unep.org/resources/publication/scientific-assessment-ozone-layer-depletion-2022>.

1501 Yamanouchi, S., Viatte, C., Strong, K., Lutsch, E., Jones, D. B. A., Clerbaux, C., Van Damme, M., Clarisse, L., and
1502 Coheur, P.-F.: Multiscale observations of NH3 around Toronto, Canada, *Atmos. Meas. Tech.*, **14**, 905–921,
1503 <https://doi.org/10.5194/amt-14-905-2021>, 2021.

1504 Zhao, X., Fioletov, V., Redondas, A., Gröbner, J., Egli, L., Zeilinger, F., López-Solano, J., Arroyo, A. B., Kerr, J.,
1505 Maillard Barras, E., Smit, H., Brohart, M., Sit, R., Ogyu, A., Abboud, I., and Lee, S. C. (2023). The site-specific primary
1506 calibration conditions for the Brewer spectrophotometer. *Atmos. Meas. Tech.*, **16**, 2273–2295.
1507 <https://doi.org/10.5194/amt-16-2273-2023>.

1508 Zhou, M., Langerock, B., Vigouroux, C., Sha, M. K., Ramonet, M., Delmotte, M., Mahieu, E., Bader, W., Hermans, C.,
1509 Kumps, N., Metzger, J.-M., Duflot, V., Wang, Z., Palm, M., and De Mazière, M.: Atmospheric CO and CH4 time series
1510 and seasonal variations on Reunion Island from ground-based in situ and FTIR (NDACC and TCCON) measurements,
1511 *Atmos. Chem. Phys.*, **18**, 13881–13901, <https://doi.org/10.5194/acp-18-13881-2018>, 2018.

1512 Zhou, M., Langerock, B., Vigouroux, C., Sha, M. K., Ramonet, M., Delmotte, M., Mahieu, E., Bader, W., Hermans, C.,
1513 Kumps, N., Metzger, J.-M., Duflot, V., Wang, Z., Palm, M., and De Mazière, M.: Atmospheric CO and CH4 time series
1514 and seasonal variations on Reunion Island from ground-based in situ and FTIR (NDACC and TCCON) measurements,
1515 *Atmos. Chem. Phys.*, **18**, 13881–13901, <https://doi.org/10.5194/acp-18-13881-2018>, 2018.

1516 Zhou, M., Langerock, B., Vigouroux, C., Sha, M. K., Ramonet, M., Delmotte, M., Mahieu, E., Bader, W., Hermans, C.,
1517 Kumps, N., Metzger, J.-M., Duflot, V., Wang, Z., Palm, M., and De Mazière, M.: Atmospheric CO and CH4 time series
1518 and seasonal variations on Reunion Island from ground-based in situ and FTIR (NDACC and TCCON) measurements,
1519 *Atmos. Chem. Phys.*, **18**, 13881–13901, <https://doi.org/10.5194/acp-18-13881-2018>, 2018.



1517 and seasonal variations on Reunion Island from ground-based in situ and FTIR (NDACC and TCCON) measurements,
1518 *Atmos. Chem. Phys.*, 18, 13881–13901, <https://doi.org/10.5194/acp-18-13881-2018>, 2018.
1519 Zhou, M., Langerock, B., Wells, K. C., Millet, D. B., Vigouroux, C., Sha, M. K., Hermans, C., Metzger, J.-M., Kivi, R.,
1520 Heikkinen, P., Smale, D., Pollard, D. F., Jones, N., Deutscher, N. M., Blumenstock, T., Schneider, M., Palm, M., Notholt,
1521 J., Hannigan, J. W., and De Mazière, M.: An intercomparison of total column-averaged nitrous oxide between ground-
1522 based FTIR TCCON and NDACC measurements at seven sites and comparisons with the GEOS-Chem model, *Atmos.*
1523 *Meas. Tech.*, 12, 1393–1408, <https://doi.org/10.5194/amt-12-1393-2019>, 2019.
1524 Zhou, M., Langerock, B., Vigouroux, C., Sha, M. K., Hermans, C., Metzger, J.-M., Chen, H., Ramonet, M., Kivi, R.,
1525 Heikkinen, P., Smale, D., Pollard, D. F., Jones, N., Velasco, V. A., García, O. E., Schneider, M., Palm, M., Warneke, T.,
1526 and De Mazière, M.: TCCON and NDACC XCO measurements: difference, discussion and application, *Atmos. Meas.*
1527 *Tech.*, 12, 5979–5995, <https://doi.org/10.5194/amt-12-5979-2019>, 2019.
1528 Zhou, M., Langerock, B., Sha, M. K., Hermans, C., Kumps, N., Kivi, R., Heikkinen, P., Petri, C., Notholt, J., Chen, H.,
1529 and De Mazière, M. (2023). Atmospheric N₂O and CH₄ total columns retrieved from low-resolution Fourier transform
1530 infrared (FTIR) spectra (Bruker VERTEX 70) in the mid-infrared region. *Atmos. Meas. Tech.*, **16**, 5593–5608.
1531 <https://doi.org/10.5194/amt-16-5593-2023>.
1532 Zhou, M., Langerock, B., Vigouroux, C., Smale, D., Toon, G., Polyakov, A., Hannigan, J. W., Mellqvist, J., Robinson,
1533 J., Notholt, K., Strong, E. Mahieu, M. Palm, M. Prignon, N. Jones, O. Garc'ia, I. Morino, I. Murata, I. Ortega, T.
1534 Nagahama, T. Wizenberg, V. Flood, K. Walker, and M. De Mazi'ere. (2024). Recent decreases in the growth rate of
1535 atmospheric HCFC-22 column derived from the ground-based ftir harmonized retrievals at 16 NDACC sites.
1536 *Geophysical Research Letters*, **51**(22):e2024GL112470. <https://doi.org/10.1029/2024GL112470>.
1537 Zuber, R., Köhler, U., Egli, L., Ribnitzky, M., Steinbrecht, W., and Gröbner, J.: Total ozone column intercomparison of
1538 Brewers, Dobsons, and BTS-Solar at Hohenpeissenberg and Davos in 2019/2020, *Atmos. Meas. Tech.*, 14, 4915–4928,
1539 <https://doi.org/10.5194/amt-14-4915-2021>, 2021.
1540 Zumkehr, A., Hilton, T. W., Whelan, M., Smith, S., Kuai, L., Worden, J., and Campbell, J. E. (2018). Global gridded
1541 anthropogenic emissions inventory of carbonyl sulfide. *Atmospheric Environment*, **183**:11